MAGNETIC ROTATION SPECTRA
OF
NITRIC OXIDE IN THE NEAR INFRARED

by

Glen Alan Mann

AN ABSTRACT

Submitted to the School for Advanced Graduate Studies of
Michigan State University of Agriculture and
Applied Science in partial fulfillment of
the requirements for the degree of

DOCTOR OF PHILOSOPHY

Department of Physics and Astronomy

1959

Approved C. A. Hause

Glen Alan Mann

ABSTRACT

Observations of the magnetic rotation spectra for the 2-0 and 3-0 vibration rotation bands at 2.7 μ and 1.8 μ, respectively, of nitric oxide have been made. Using a multiple traverse cell of the White type, absorbing paths of .1 to 8 meter-atmospheres were used. An air cooled solenoid capable of giving 2,400 gauss was constructed and the multiple traverse cell was placed in the central third of the solenoid inside a brass tube which held the gas.

The magnetic rotation seen in the 2-0 band was limited to the R and Q branches and only the direction of rotation was determined for the R branch. For the 3-0 band, magnetic rotation was seen for the P, Q and R branches. In the P and R branches only the direction of rotation for the components was determined. The Q branch showed large rotations and it was possible to determine the frequency of the rotated lines. The frequencies agree very well with those found in the absorption spectrum. One line appears in magnetic rotation at a frequency predicted by the constants for nitric oxide, but this line is not observed in absorption due to the overlapping of the Q branches.

A small rotation is observed for the first R branch line in the 3-0 band. Any magnetic moment associated with the molecule at such a low value of rotational energy is of the order of .05 μ_0. Magnetic rotation spectra, therefore, may furnish a method of detecting molecules with small magnetic moments.

Nitric oxide has a $^2\pi$ ground state. The 2-0 and 3-0 bands consist of two bands, one for $^2\pi_{1/2} - {}^2\pi_{1/2}$ transitions and another for $^2\pi_{3/2} - {}^2\pi_{3/2}$ transitions. The magnetic rotation spectra shows that all transitions involving the $^2\pi_{1/2}$ state are rotated in a negative sense while those involving $^2\pi_{3/2}$ are rotated in a positive sense, viz. negative rotation is a counter-clockwise rotation as one looks against the incoming light and positive rotation is clockwise.

MAGNETIC ROTATION SPECTRA OF NITRIC OXIDE IN THE NEAR INFRARED

by

Glen Alan Mann

A THESIS

Submitted to the School for Advanced Graduate Studies of
Michigan State University of Agriculture and
Applied Science in partial fulfillment of
the requirements for the degree of

DOCTOR OF PHILOSOPHY

Department of Physics and Astronomy

1959

Approved C. D. Hause

ACKNOWLEDGEMENTS

The author wishes to express his sincere thanks to Dr. C. D. Hause for suggesting the problem and for his considerable aid and guidance throughout the project. It was through his and Dr. T. H. Edwards' efforts that a grant was obtained from the National Science Foundation to support this project. The author wishes to express his thanks to the National Science Foundation for its grant (NSFG-5959) to aid the research.

TABLE OF CONTENTS

LIST OF FIGURES

LIST OF TABLES

INTRODUCTION

The magnetic rotation spectrum of a gas is the spectrum of the radiation transmitted through crossed polarizing elements when the magnetized gas is placed between them so that the light traverses the gas in the direction of the magnetic field. Thus, the spectrum is essentially an enhanced Faraday Effect closely associated with the longitudinal Zeeman Effect.

Magnetic rotation spectra have been observed in monatomic and diatomic gases. Macaluso and Corbino[1] discovered the effect in monatomic gases. The magnetic rotation spectrum of a diatomic gas, sodium vapor, was first observed by R. W. Wood[2]. Magnetic rotation spectra have also been observed by Righi[3], Loomis[4], and Carroll[5]. All of these observations were made on the diatomic vapors of alkali metals, and iodine, bromine, and bismuth. These spectra were confined to the photographic region and were associated with electronic band systems in which the upper state alone possessed magnetic properties, or the upper state was perturbed by some close lying state which exhibited magnetic characteristics.

Since magnetic rotation is closely associated with the Faraday Effect, which in turn depends upon the longitudinal Zeeman Effect, magnetic rotation spectra will only

be observed for those transitions which show an appreciable Zeeman splitting. Even though the rotation of the plane of polarization becomes abnormally large at absorption frequencies, the amount of light transmitted through the analyzer is relatively small. The magnetic rotation spectra that have been observed required exposures of several hours. These spectra were associated with electronic transitions and the only lines that were seen occurred at band heads and low J values. The reason for this is that at band heads there are several absorption lines very close together, and the rotations for the individual lines all add together giving a large rotation. The low J value terms sometimes observed are favored because of their relatively large Zeeman splittings.

Since these spectra were taken, detection techniques in the infrared have been improved by the introduction of Lead Sulphide detectors. Gratings are at present being ruled which give energy distribution curves with maxima in the near infrared. The introduction of multiple traverse cells, such as the White type, give large absorbing paths without the need for high pressures so that pressure broadening need not be the limit of resolution. It was for these reasons and also because the NO molecule has both upper and lower states with magnetic characteristics

that it was thought the magnetic rotation spectra of nitric oxide in a single vibration-rotation band might be observable.

THEORY

Hund's Coupling Cases (a) & (b)

The electronic states and rotational energies of a diatomic molecule are classified by the manner in which the angular momenta of the electrons are coupled and the way in which they are coupled to the other motions of the molecule. Different schemes of coupling of the internal angular momenta were first considered by Hund. We will be concerned only with the types of coupling known as Hund's case (a) and case (b), and the coupling intermediate between (a) and (b).

In Hund's case (a), it is assumed that the interaction of the nuclear rotation with the electronic motion is very weak, but the electronic motion itself is coupled very strongly to the line joining the two nuclei. The electronic orbital angular momentum (L) is coupled very strongly with the electronic spin (S) and their projections along the internuclear axis, Λ and Σ respectively, combine to form a resultant Ω which in turn is coupled with the angular momentum N of nuclear rotation to form the resultant total angular momentum J. The vector J is a constant in magnitude and direction. Ω and N precess about J. At the same time L and S precess about the internuclear axis.

In Hund's case (a), the precession of L and S about the internuclear axis is assumed to be very much faster than the precession of Ω and N about J.

In Hund's case (b), the electron spin S is uncoupled from the electronic orbital angular momentum L. That is, the orbital angular momentum L is coupled to the internuclear axis and combines with the angular momentum N of the nuclear rotation to form a vector K. The angular momentum K combines with the electron spin S to form the total angular momentum J which is constant in magnitude and direction. Thus, in case (b), we have S and K precessing about J while Λ and N precess about K. In Hund's case (b) the precession of K and S about J is assumed to be very slow compared with the precession of Λ and N about K[6]. Vector diagrams of these coupling schemes are shown in Figures 1 and 2.

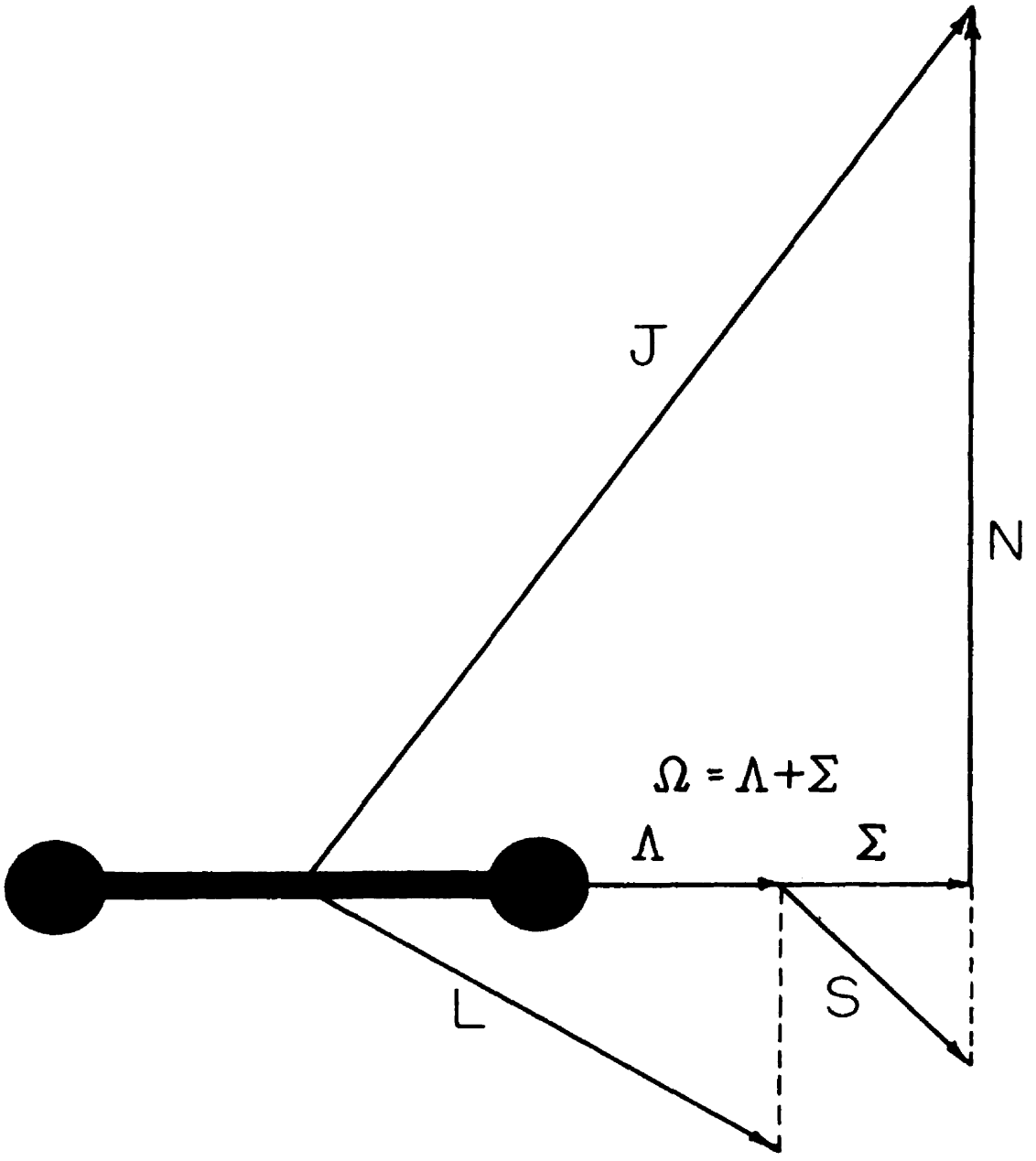

HUND'S COUPLING CASE "A"

FIGURE 1

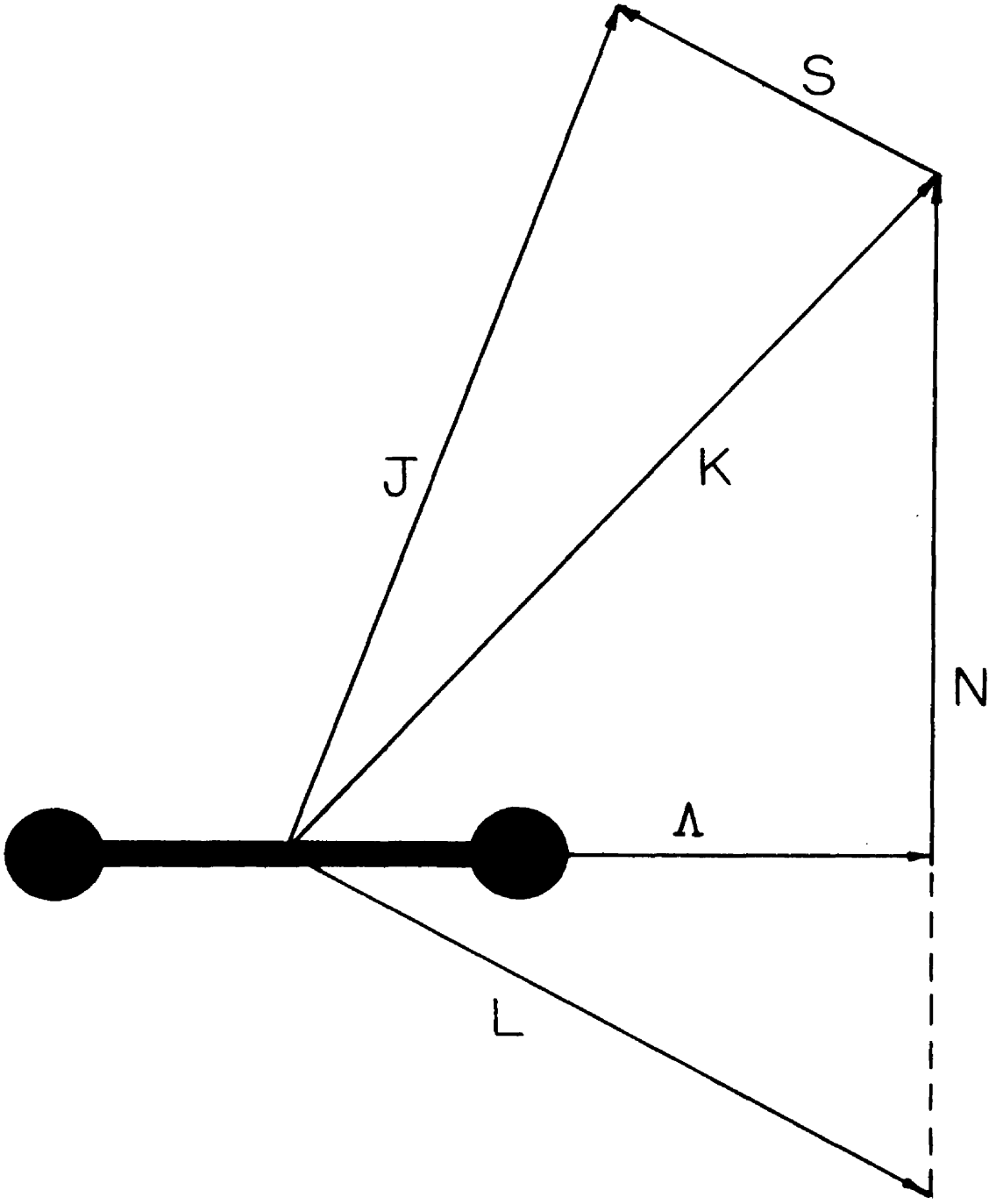

HUND'S COUPLING CASE "B"

FIGURE 2

Intermediate Coupling

Hund's coupling cases represent idealizations which are never fully realized, although they frequently represent a good approximation to the coupling for the molecule. It sometimes occurs that with increasing rotation, the coupling of a molecule may change from one idealized case to another.

We want now to look at the transition from case (a) to case (b) coupling which is called spin uncoupling. If one assumes a molecule coupled according to case (a) for small rotational values, then S is coupled with Λ along the internuclear axis. S precesses around Λ while the molecule rotates. As the rotation increases, its value approaches that of the precessional frequency of S, and if the rotation of the molecule increases still more the influence of the molecular rotation will become the predominant one. When this happens, S can no longer couple itself with Λ along the internuclear axis. Instead, Λ will combine with N to form a resultant K, which then combines with S to give the total angular momentum of the molecule J, which is case (b) coupling.

The rotational term values for the components of doublet states have been obtained by Hill and Van Vleck[7] for any strength of coupling between Λ and S, but neglecting

the coupling between K and S. They obtained,

$$F_1(J) = B_v\left[\left(J+\tfrac{1}{2}\right)^2 - \Lambda^2 - \tfrac{1}{2}\sqrt{4\left(J+\tfrac{1}{2}\right)^2 + Y(Y-4)\Lambda^2}\right] - D_v J^4$$

$$F_2(J) = B_v\left[\left(J+\tfrac{1}{2}\right)^2 - \Lambda^2 + \tfrac{1}{2}\sqrt{4\left(J+\tfrac{1}{2}\right)^2 + Y(Y-4)\Lambda^2}\right] - D_v (J+1)^4$$

where $Y = \frac{A}{B_v}$, where A, the coupling constant, is the separation of the two components and is determined from the equation $T_e = T_o + A\Lambda\Sigma$ where T_e is the electronic energy of a multiplet term and T_o the electronic energy when spin is neglected. B_v is inversely proportional to the moment of inertia of the molecule about a line perpendicular to the figure axis, $B_v = \frac{h}{8\pi^2 c I_B}$. The type of coupling may be inferred from the value of Y. For A much greater than B_v, that is large Y, the coupling is close case (a). For A about equal to or smaller than B_v, that is Y small, around 1, the coupling is near case (b). For Y equal to 0 or 4, the second term in the square root is zero and the coupling is actually case (b). $F_1(J)$ is the term series for which $J = K + 1/2$ and $F_2(J)$ is the term series for which $J = K - 1/2$, that is $F_1(J)$ and $F_2(J)$ are the term series for $^2\pi_{1/2}$ and $^2\pi_{3/2}$, respectively.

Figure 3 shows the shift of energy levels for the transition of a regular $^2\pi$ state when the coupling changes from case (a) to case (b).

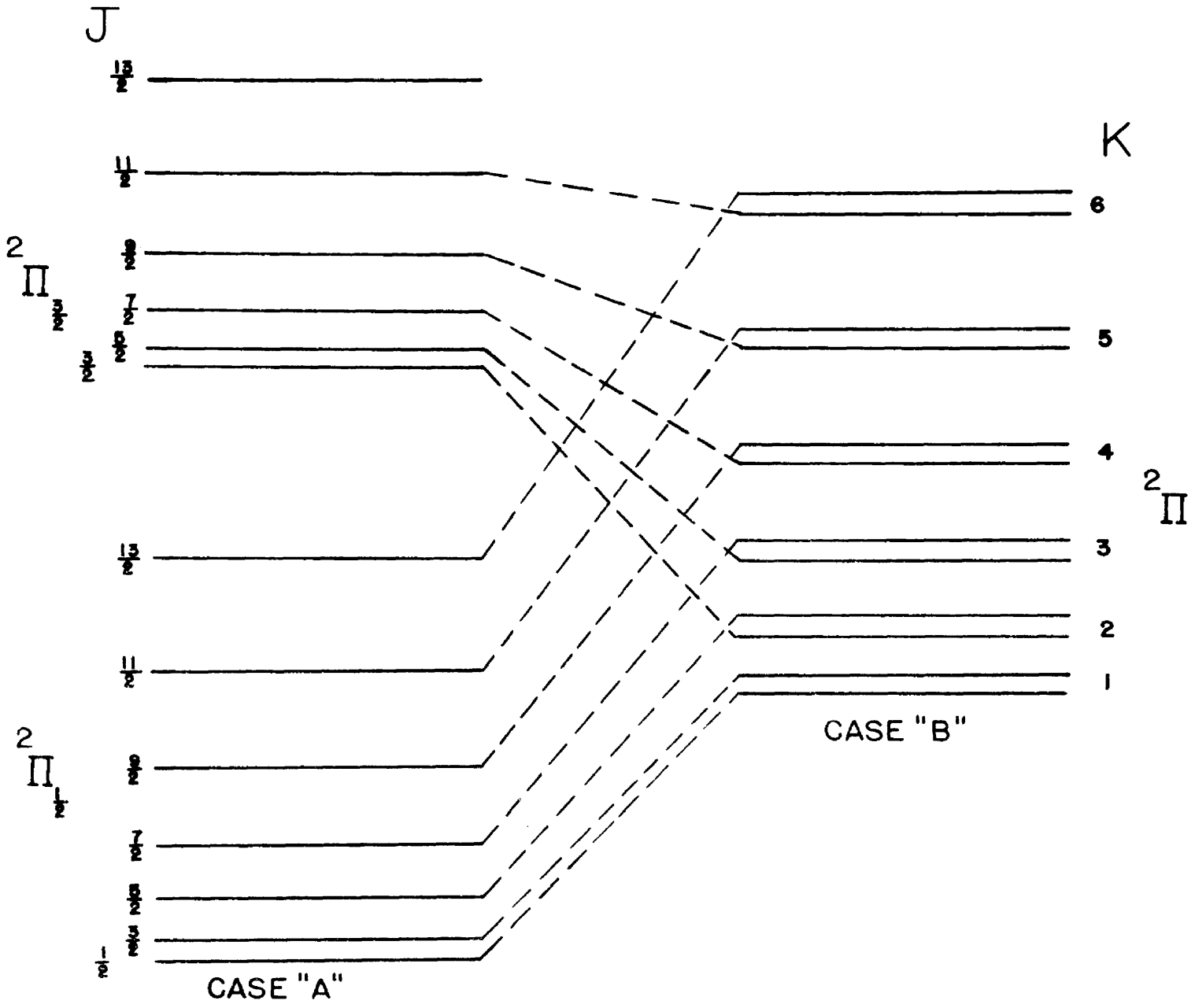

TRANSITION FROM CASE "A" TO CASE "B" FOR A REGULAR $^2\Pi$ STATE

FIGURE 3

Nitric Oxide

Nitric oxide is a colorless, slightly heavier-than-air gas which is toxic in very small quantities and poisonous in moderate quantities. It is a diatomic molecule which has a molecular weight of 30.01 and whose atomic number is 15. Its normal freezing and boiling points are -163°C and -152°C, respectively.

Nitric oxide is the only chemically stable diatomic molecule having an odd number of electrons, indicating a resultant electron spin. The projection of the electronic spin angular momentum along the internuclear axis, Σ, must be half-integral. Since this spin vector can combine with Λ, the projection of L, along the internuclear axis in one of two ways, the ground state of NO must be a doublet state.

The type of electronic state, that is $\Sigma, \Pi, \Delta \ldots$, is determined by the electron configuration of the molecule. The electron configuration for NO is

$$K K (\sigma_g 2s)^2 (\sigma_u 2s)^2 (\sigma_g 2p)^2 (\pi_u 2p)^4 \pi_g 2p \quad (8)$$

The fifteenth electron is a π electron. This means that the ground state will be a π state. Thus, the ground state of nitric oxide is $^2\pi_{1/2}$ and $^2\pi_{3/2}$.

Dispersion

Dispersion can be defined as the change in the index of refraction of a medium with the frequency of transmitted radiation. When the index of refraction is smaller for long wave lengths than it is for the shorter wave lengths, we say the dispersion is normal. Normal dispersion can be explained by assuming, for transparent materials, absorption frequencies in the ultraviolet due to electrons and absorption frequencies in the infrared due to ions. In normal dispersion formulas a term appears in the denominator which involves differences between the squares of an absorption frequency and the frequency of the incoming radiation so that when the radiation frequency is equal to this absorption frequency, the value of the index of refraction for the material becomes discontinuous. Whenever the index of refraction is greater for longer wave lengths than it is for shorter wave lengths, the dispersion is called anamolous. This takes place in general at absorption frequencies. It is anamolous dispersion in which we are primarily interested.

In order to overcome the difficulties in the expression for normal dispersion which arise at absorption frequencies, one introduces a term similar to the damping term in the equation for a damped harmonic oscillation.

This term makes the theoretical value for the index of refraction remain finite when one passes through an absorption frequency. One can use either the mechanical or Helmholtz approach, the electro-magnetic approach or the quantum mechanical approach. In any case, one obtains similar relations between the index of refraction and the frequency. The difference arises in the meaning attached to the symbols.

In the mechanical and electro-magnetic approaches, one considers forced oscillations of the electrons and the ions by the incoming light wave and the natural oscillations of the electrons and the ions in the material. In the quantum mechanical case one considers the frequency of the incoming radiation, the frequency corresponding to transitions of electrons from one energy state to another, and the transition probabilities. The quantum mechanical representation of the index of refraction as a function of frequency for normal dispersion is

$$n^2 = 1 + \frac{Ne^2}{\pi m}\left[\sum \frac{-2 A_{jk} g_{jk}}{\nu_{jk}^2 - \nu^2}\right] \qquad (9)$$

where N is the number of dispersion electrons per unit volume, e is the electronic charge, m is the electronic mass, A_{jk} is the induced transition probability from

state j to k by the frequency ν, g_{jk} is the spontaneous transition probability from the state j to k, ν_{jk} is the frequency difference between the states j and k, and ν is the frequency of the incoming radiation.

A classical expression for the index of refraction for anamolous dispersion and the absorption that takes place at the same frequency is given by the following expressions:

$$n^2(1-\alpha\ell^2) = n_m^2 - \frac{a\,x}{x^2+g^2(1+x)}$$

for the index of refraction, and

$$2n^2\alpha\ell = \frac{a\,g\sqrt{1+x}}{x^2+g^2(1+x)} \qquad (10)$$

for the absorption where n_m is the average contribution to the index by all the other resonance frequencies except ω_0, a is $\frac{Ne^2}{m\epsilon_0\omega_0}$, ϵ_0 is the dielectric constant for vacuum, g is the damping constant, a number much less than one to make the absorption peak sharp, $\alpha\ell$ is the absorption coefficient for the medium, and $x = \frac{\omega^2-\omega_0^2}{\omega_0^2}$ where ω_0 is the natural frequency of the dispersion electron, and ω is the frequency of the incoming radiation.

Zeeman Effect

The Zeeman Effect is the effect an external magnetic field has on the radiation of an atom or molecule. When the radiation is observed perpendicular to the field the effect is called the transverse Zeeman Effect. The longitudinal Zeeman Effect is that observed when one looks along the direction of the magnetic field. The presence of the magnetic field removes the degeneracy of the space quantization by giving a preferred direction around which the total angular momentum of the molecule can rotate.

The classical Zeeman Effect is obtained by reducing the motion of the electrons in the molecule to three compound motions, in each of which the binding is assumed to be elastic: one is a linear harmonic motion along the field direction and the other two are uniform circular motions in opposite directions in a plane perpendicular to the field direction. We will concern ourselves only with the longitudinal Zeeman Effect. In the normal pattern, only two lines are seen and these lines are right and left circularly polarized. Only two lines are seen since, classically, there will be no radiation emitted along the field by the motion of the electron which is vibrating parallel to the field direction. The two lines that are

seen are circularly polarized since they come from the two circular motions perpendicular to the field. One of these has a higher and the other a lower frequency than the line seen without the field, since one of the rotations is aided by the magnetic field while the other rotation is retarded by the field. The shift in frequency from the field free case is given by $W - W_0 = \mu_0 H$ where μ_0 is the Bohr magneton equal to $\frac{eh}{4\pi mc}$, and is referred to as $\Delta\nu_N$.

Anamolous Zeeman Effect

In a magnetic field the total angular momentum J of the molecule is space quantized such that the component of J along the field is $M\hbar$ where $M = -J, -J+1 \ldots J$. The states with a different M have somewhat different energies. The energies are given by $W = W_0 - \bar{\mu}_H H$, where W_0 is the energy of the molecule in the absence of the field, $\bar{\mu}_H$ is the mean value of the component of the magnetic moment in the field direction and H is the value of the field. In order to determine the Zeeman Effect for a molecule one must evaluate $\bar{\mu}_H$ for that particular molecule. If the molecule is coupled according to Hund's case (a), the value of $\bar{\mu}_H$ is found to be $\bar{\mu}_H = \frac{(\Lambda+2\Sigma)(\Lambda+\Sigma) M \mu_0}{J(J+1)}$ where μ_0 is the Bohr magneton. If the molecule is coupled according to Hund's case (b) the value of $\bar{\mu}_H$ is given by

$$\bar{\mu}_H = \frac{\Lambda^2 M_K \mu_0}{K(K+1)} + 2 M_S \mu_0 .$$

Since most molecules are neither pure case (a) nor pure case (b), one must obtain an expression for $\bar{\mu}_H$ or the Zeeman splitting for the intermediate coupling case. This has been done by Hill[11] and has been used by Crawford[12]. Using the equations given by Crawford, Figure 4 shows the maximum Zeeman splitting, $M = \pm J$, as a function of J or K for nitric oxide in terms of $\Delta\nu_N$, the splitting for the

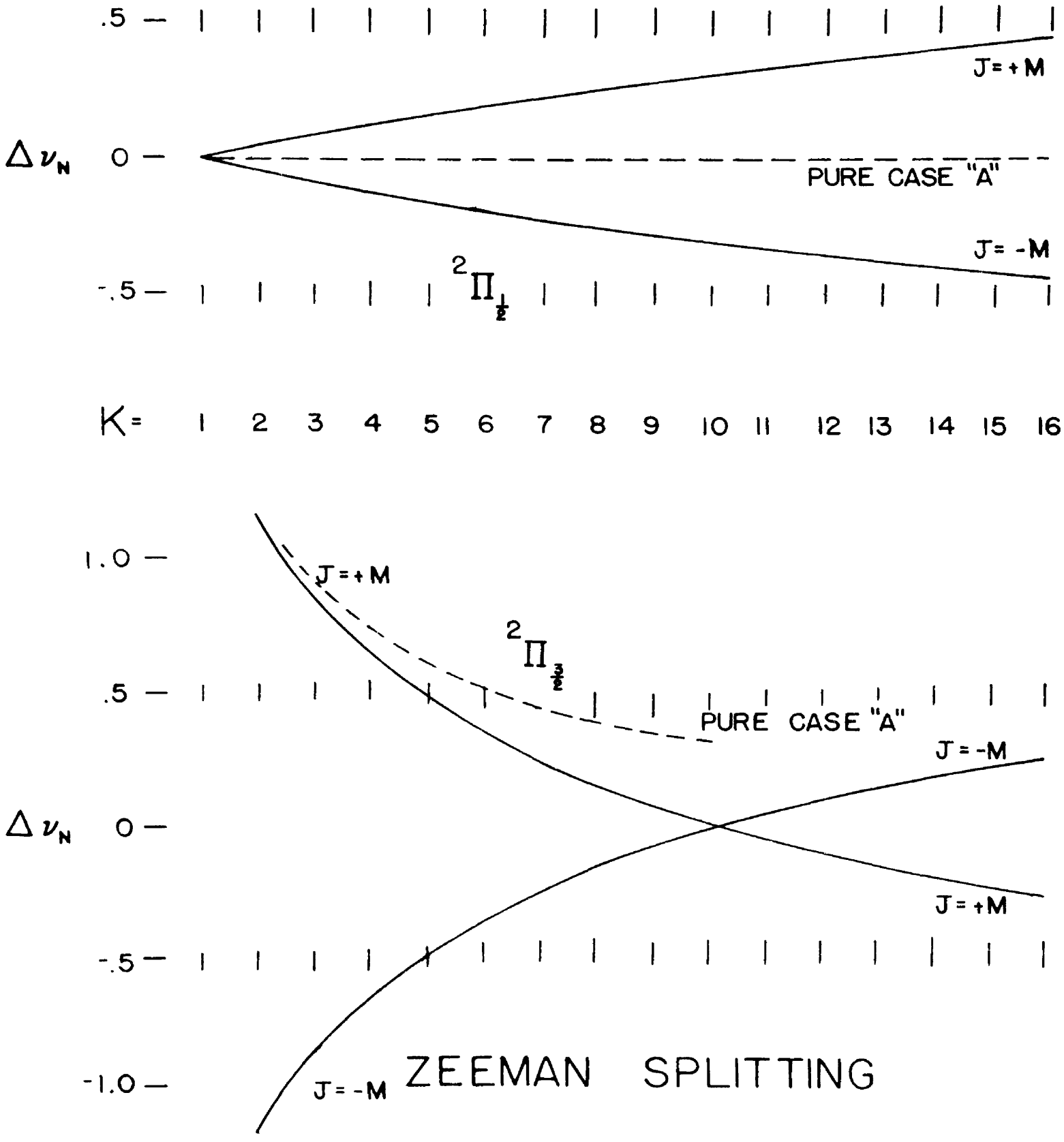
.5
J = +M
$\Delta \nu_N$ 0
PURE CASE "A"
J = -M
-.5
$^2\Pi_{\frac{1}{2}}$
K = 1 2 3 4 5 6 7 8 9 10 11 12 13 14 15 16
1.0
J = +M
$^2\Pi_{\frac{3}{2}}$
.5
PURE CASE "A"
J = -M
$\Delta \nu_N$ 0
J = +M
-.5
-1.0
J = -M
ZEEMAN SPLITTING
FOR NO v = 0, 1, 2, 3

FIGURE 4

normal Zeeman Effect. The curves in Figure 4 also show that with increasing rotation the coupling scheme for NO goes from case (a) to case (b). For the upper curve at $K = 1$, $J = 1/2$, there is no splitting, meaning that S is antiparallel to Λ, case (a). As the rotation of the molecule increases S uncouples from Λ and becomes coupled to the vector K, case (b). Since the condition $J = +M$ has the greater energy, S is parallel to K. In the lower curve for small values of J, S is parallel to Λ or nearly so since $J = +M$ has the higher energy, case (a). As the rotation increases a point is reached where the sum of Λ and S is zero resulting in no magnetic moment for the molecule. This occurs at about $K = 10$. As the rotation increases still more S becomes coupled to K, case (b), and is actually antiparallel to K, or nearly so, since $J = -M$ has the higher energy.

For the longitudinal Zeeman Effect the selection rule for transitions is $\Delta M = \pm 1$. The transition $\Delta M = +1$ gives lines shifted to higher frequencies and left circularly polarized, while transitions of $\Delta M = -1$ gives lines shifted to lower frequencies and right circularly polarized.

Figure 5 indicates the appearance of the Zeeman components for several values of J or K, depending on whether the molecule approximates case (a) or case (b)

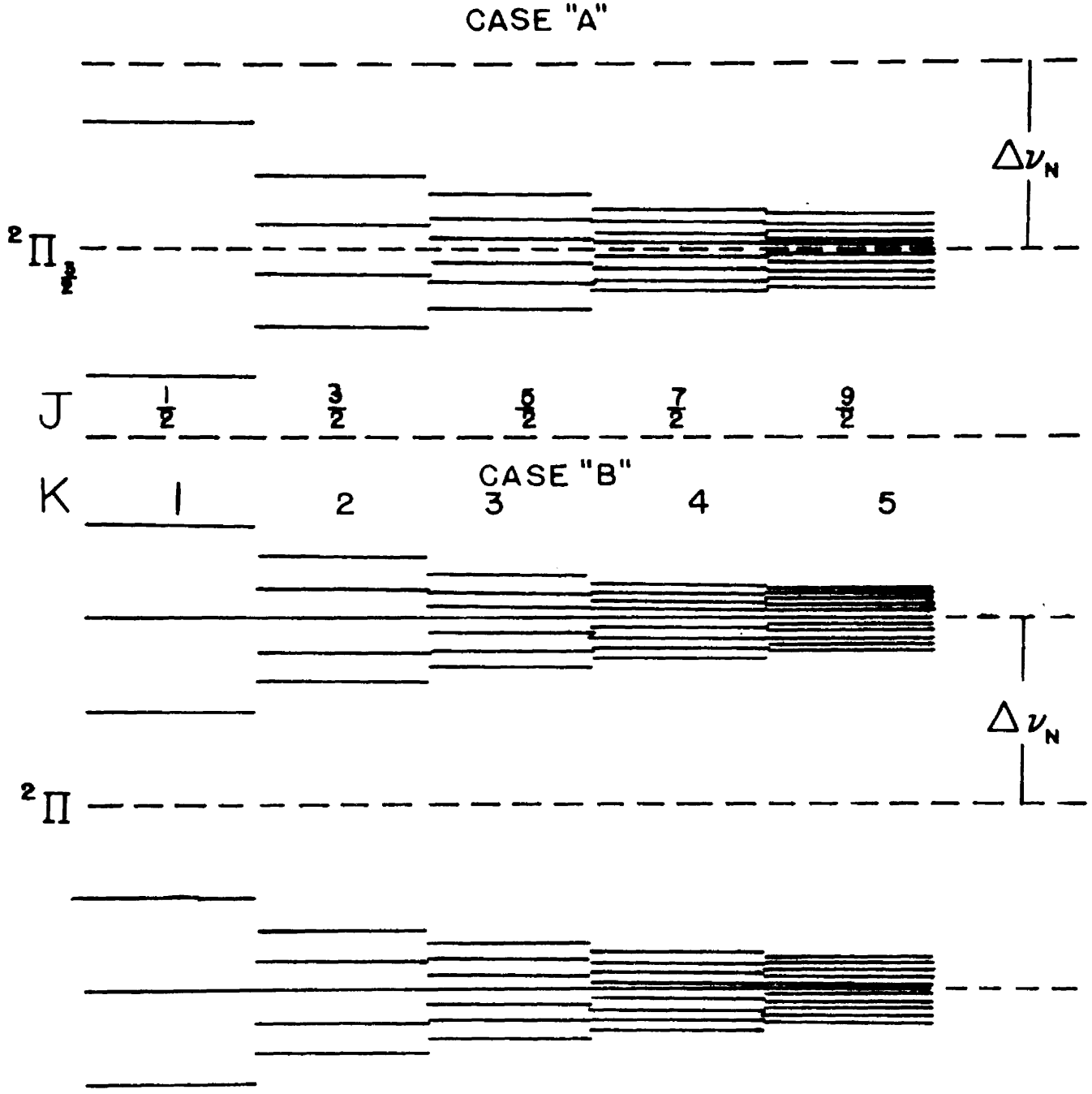

ZEEMAN SPLITTINGS AND COMPONENTS

FIGURE 5

coupling. The separation between components is given only as a function of the various M values divided by $J(J+1)$ or $K(K+1)$ and it is assumed that the other terms are a constant. For the case (a) type coupling of the $^2\pi_{1/2}$ state, the quantity $\Lambda + 2\Sigma = 0$, so that this substate will not show any splitting. Thus, only the $^2\pi_{3/2}$ state is shown. It can be seen that for case (a) splitting the number of components is $2J+1$ and as J increases, the separation between components decreases rapidly. For high J values there is practically no splitting. For case (b) coupling the number of components is $2(2K+1)$ and as K increases the separation between components rapidly decreases. For large K values the components are no longer resolved and the resulting splitting is practically that of the normal Zeeman Effect.

With the magnetic fields normally employed, usually around 20,000 gauss, the Zeeman components of the individual lines in a vibration-rotation band are not resolved except for low J values and general broadening for higher J values. A picture of the Zeeman Effect in the 3-0 band of NO for H = 2,400 gauss is shown in Figure 22. The only noticeable change in the appearance of the spectrum is a broadening of the Q branch.

The Faraday Effect

The Faraday Effect is observed by passing plane polarized light through a substance which has been placed in a magnetic field and observing the transmitted radiation through an analyzer when the direction of propagation of the radiation is along the magnetic field. The Faraday Effect is observed in all transparent media. The Effect is usually small since most transparent substances are diamagnetic. It is most easily observed in a paramagnetic medium near natural absorption frequencies for that medium.

When the magnetic field is turned on there will be for each absorption frequency without the field at least two absorption frequencies, one for right and the other for left circularly polarized light according to the theory of the Zeeman Effect. For each of these directions of rotation, one may draw an absorption curve and a dispersion curve. A total dispersion curve may be drawn for the whole region. This is shown in Figure 6. In this figure, one of the dispersion curves is n_+ and the other is n_-, depending on which absorption curve belongs to the right circular or left circular component. The total dispersion curve at the bottom of the page is then either $n_+ - n_-$ or $n_- - n_+$. From this drawing one notices that outside

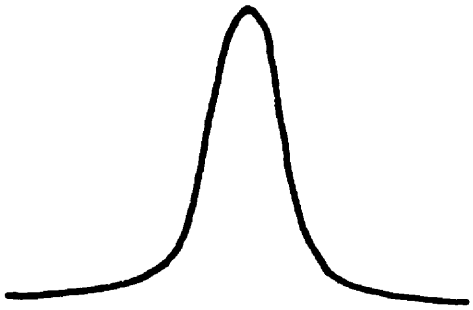

ABSORPTION CURVE

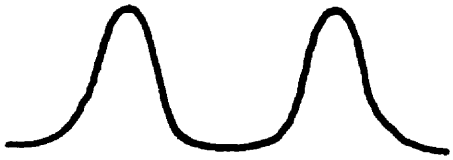

ZEEMAN COMPONENTS

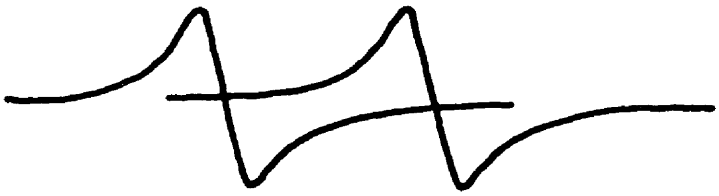

DISPERSION CURVES

RESULTANT DISPERSION CURVE

FIGURE 6

the absorption lines one of the circular polarized radiations travels faster than the other, while between the absorption frequencies the reverse is true. This means that the plane of polarization will be rotated in one direction outside of the two absorption frequencies, while the plane of polarization will be rotated in the opposite direction between the absorption frequencies when the two circular components recombine to form a plane polarized beam upon emergence from the field region.

An examination of the resultant dispersion curve shown in Figure 6 indicates that rotation would probably only be detected outside of the absorption lines. The rotation which occurs between the two Zeeman absorption components will probably be hidden by the absorption that takes place at these frequencies. For this reason a balance must be reached between the amount of absorption and the amount of rotation. If the absorption is increased by increasing the pressure of the gas, then a point will be reached at which the absorption line will mask all of the rotation. At this pressure the absorption line will be broad enough to cover the rotation which normally could be detected just outside of the frequencies of the Zeeman absorption components.

In Figure 6 it has been assumed that the splitting

of the absorption line results in two Zeeman components of equal intensity. It may happen that the intensities of the two components in the magnetic field are not equal. In this case then the two dispersion curves will not be the same and the resultant dispersion curve which is the difference of the two individual dispersion curves will no longer be symmetric as shown in Figure 6, but will be assymmetric about the field free absorption frequency. The angle of rotation can be shown to be $\chi = -\frac{\pi \ell}{\lambda}(n_+ - n_-)$ where ℓ is the path length in the medium, λ is the wave length of the radiation, and $n_+ - n_-$ is the difference in the indices of refraction for right and left circularly polarized light. The above is a description of how one line is formed for a magnetic rotation spectrum.

The Faraday Effect, unlike substances possessing natural rotary dispersion, is increased when the radiation is reflected and sent back through the magnetized substance. The magnitude of the rotation of the plane of polarization for the Faraday Effect is proportional to the length of the sample in the magnetic field and to the field strength. The constant of proportionality is called the Verdet Constant. This constant is frequency dependent. It assumes abnormally large values when one passes through a magnetic absorption frequency for a given material.

Serber[20] has developed a general expression for the Verdet constant occurring in the Faraday Effect for diatomic molecules. He obtains the following expressions:

$$V = \sum_{n'} \left\{ \frac{\nu^2 A(nn')}{(\nu(n'n)^2 - \nu^2)^2} + \frac{\nu^2 B(nn')}{\nu(n'n)^2 - \nu^2} + \frac{\nu^2 C(nn')}{T(\nu(nn')^2 - \nu^2)} \right\}$$

The term which is most important when one is near an absorption frequency is $\frac{\nu^2 A(nn')}{(\nu(n'n)^2 - \nu^2)^2}$.

Serber has found for this term that the Verdet constant can be given as the following:

$$V = 2CB \sum_{mm'} \frac{\nu^0(n'n)\,\nu'(n'm';nm)\left[P_x^0(nm;n'm')\,P_y^0(n'm';nm)\right]}{(\nu^2 - \nu^0(n'n)^2)^2}$$

where $\nu^0(n'n)$ is the absorption frequency, $\nu'(n'm';nm)$ is the Zeeman frequency shift, B is $N/\sum_n e^{-W_n/kT}$, C is $\frac{4\pi^2\nu^2 i}{ch}$, and the P_x^0 and P_y^0 are the unperturbed transition probabilities for a change in the x and y components of the electric moment, and $\left[P_x^0(nm;n'm')\,P_y^0(n'm';nm)\right]$ stands for $P_x^0(nm;n'm')\,P_y^0(n'm';nm) - P_y^0(n'm';nm)\,P_x^0(nm;n'm')$.

This, then, says that near an absorption frequency the rotation depends only on the magnitude of the Zeeman splitting and the amplitude of the absorption without the field.

APPARATUS

The vacuum infrared grating spectograph used in this work was designed by Dr. R. H. Noble[13]. It is of the Pfund pierced flat type. The optical alignment of this spectograph has been outlined by R. G. Brown[14]. A schematic diagram (Figure 7) shows the path of the radiation through the spectograph.

The spectograph is arranged to allow two light beams to traverse the monochrometer section at the same time. One beam goes to the Lead Sulphide detector and the other is sent to a Fabry-Perot Interferometer. The Edser-Butler bands produced by sweeping the interferometer with continuous light are detected by a photomultiplier and recorded. These band contours are used for calibration. This system is referred to as the Fringe Calibration System and is explained in detail by B. H. Van Horne[15].

A 300 watt concentrated zirconium arc was used for the infrared source and a 100 watt zirconium arc was used to obtain the fringe calibration. A Lead Sulphide detector cooled to -50°C was used to detect the infrared radiation coming from the monochrometer section of the spectograph.

In order to obtain suitable absorbing paths, a multiple traverse cell of the White type was used. The

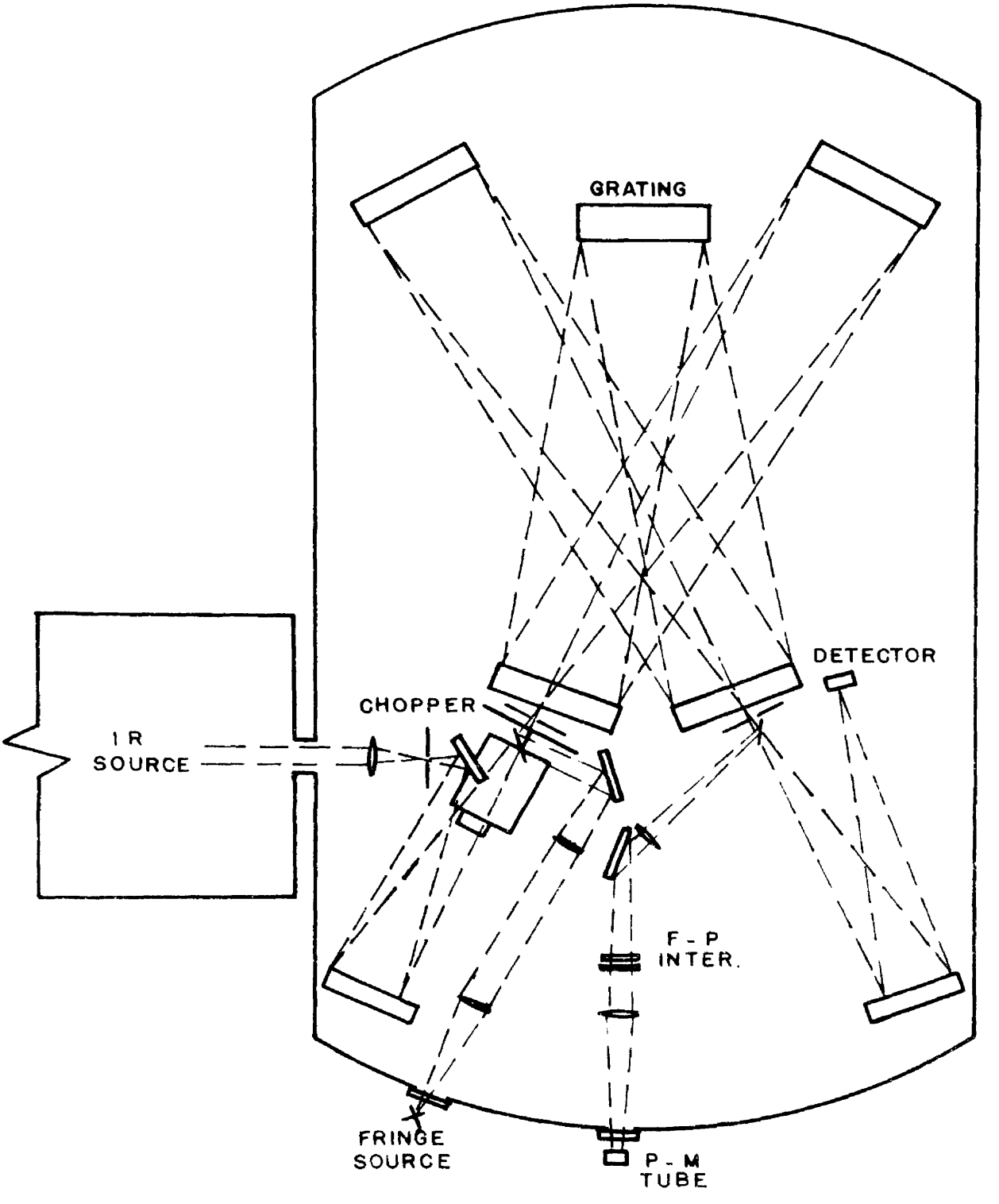

SPECTROGRAPH

FIGURE 7

cell was adjusted for 24 traversals, giving a total path of eight meters, and the pressure of NO was varied from 1 to 56 cm of mercury. This multiple traverse cell was placed inside a brass cylinder which was fitted with windows to allow the radiation to enter and leave the tube after multiple reflections in the White cell. The brass tube was then inserted in an air cooled solenoid. The multiple traverse cell was placed in the central third of the solenoid.

The solenoid consists of 36 pancake windings of insulated copper strips 1/2 inch wide and 1/16 of an inch thick. Each coil contains 90 turns. The total solenoid is 82 cm in length, which means the solenoid has 3,950 turns per meter. The 36 coils were all connected in series giving a total resistance of about 4.2 ohms. The magnetic field in the center and at places covering the central third of the solenoid was measured by nuclear magnetic resonance techniques. The variation of the field in the central third of the solenoid was not greater than 5% of the value of the field at the center. The value of the magnetic field at the center of the solenoid with a current of 38 amperes was measured as 1,650 gauss. If one compares this value with the one obtained by using the formula for an infinite solenoid, the value for the actual

solenoid is 87% of that for the theoretical infinite solenoid. Magnetic rotation spectra were obtained with fields of 2,400 gauss which meant there was a current of 55 amperes in the solenoid. The completed solenoid was placed on an aluminum frame to match the height of the spectograph bed. A picture of the completed solenoid is shown in Figure 8. A schematic diagram (Figure 9) shows the light path from the source through the absorption cell and up to the entrance slit of the spectograph.

Two vibration-rotation bands of NO were investigated -- the 2-0 band at 2.7μ and the 3-0 band at 1.8μ. For the 3-0 band the polarizers used were type HR polaroids from the Polaroid Corporation. These transmit about 40% of the incident radiation at 1.8μ when both polaroids are used with their axes parallel and almost 0% when their axes are crossed. These polaroids are in the form of plastic laminations.[16]

For the 2-0 band, multiple plates of silver chloride set at Brewster's angle for 2.7μ were used. These polarizers were loaned to us by Professor C. W. Peters of the University of Michigan Physics Department.

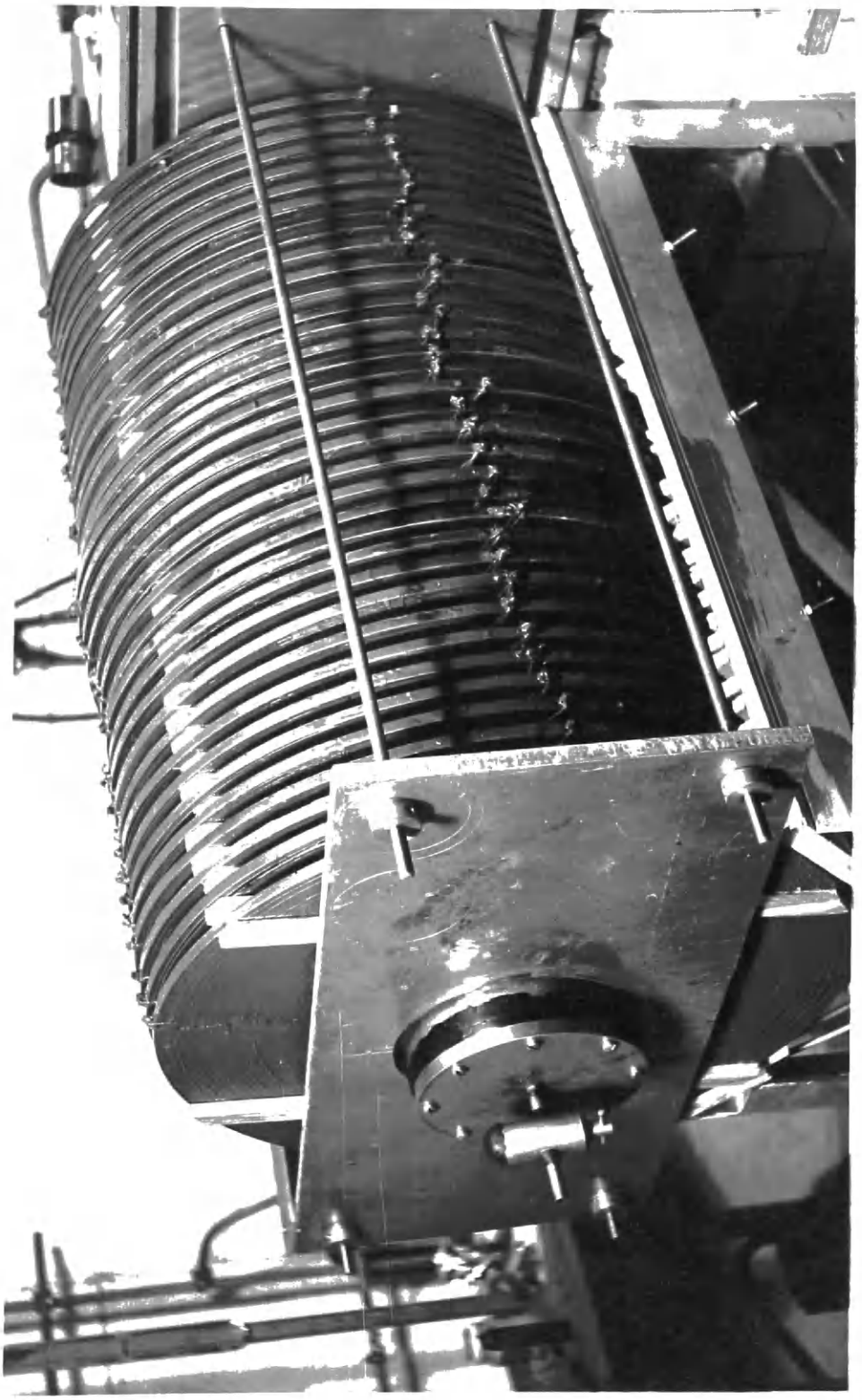

Figure 8

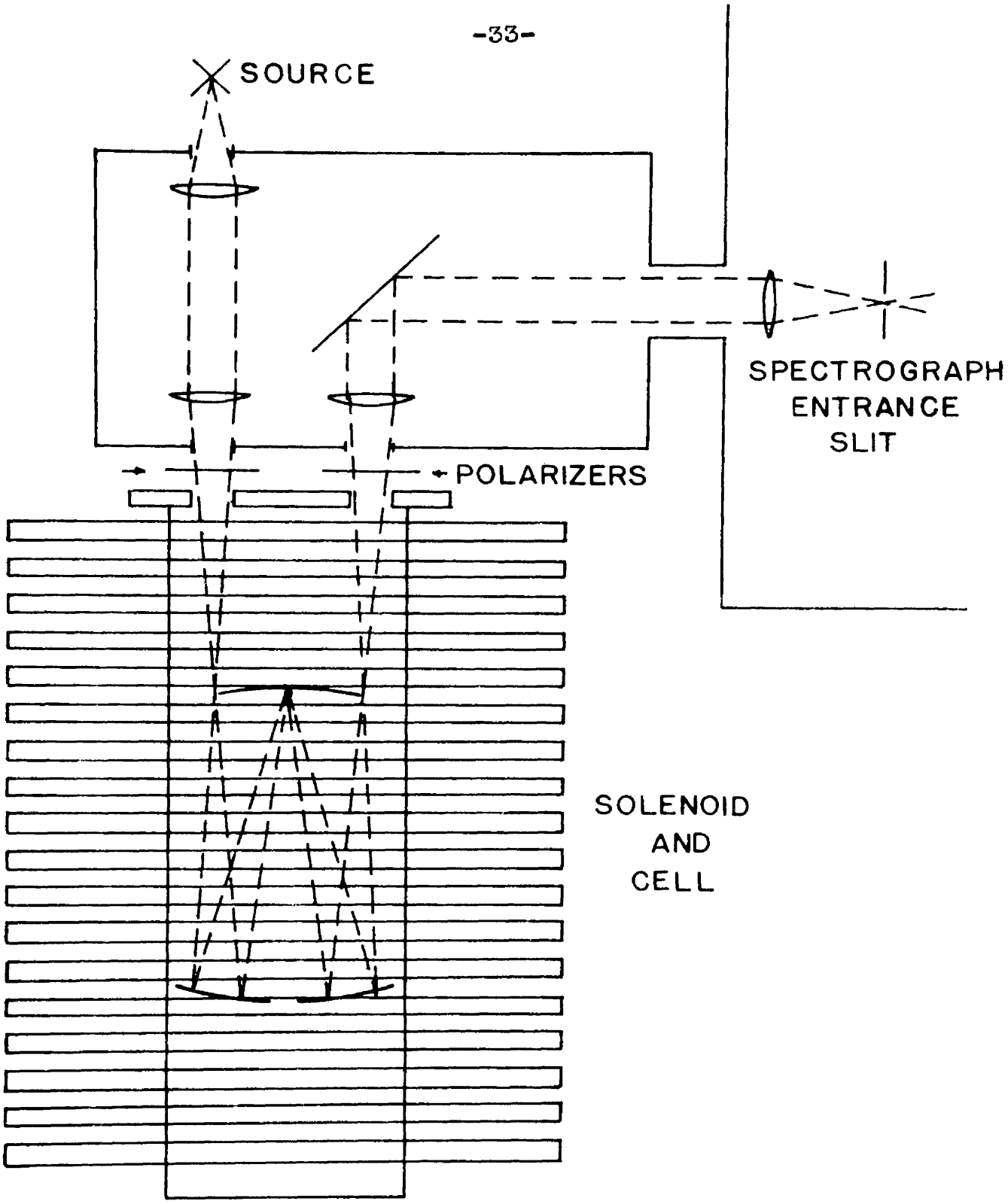

FORE - OPTICS

FIGURE 9

EXPERIMENTAL DETAILS

General

Since the amount of energy reaching the detector of the spectograph is dependent upon the angle the electric vector makes with the rulings of the grating, the analyzer was placed in position first and rotated until a maximum signal was obtained. When this position was found, the analyzer was not touched again. Both the polarizer and analyzer had an angular scale and pointer so that the angle of rotation from the crossed position could be measured.

The magnetic rotation spectra were obtained as a function of the angle between the planes of polarization of the polarizer and analyzer. It was decided to call the angle between the polarizer and analyzer 0^{o} when they were in the crossed position since neither the rotation in a plus or minus direction would be aided or retarded in this case. A rotation of the polarizer in a clockwise direction as one looks against the incident radiation was called a positive rotation. A rotation of the polarizer in a counter-clockwise direction was termed a negative rotation. The magnitude of the rotation is given by the number of degrees the polarizer is rotated away from the crossed position.

The direction and magnitude of rotation for a given line can thus be determined. As an example, consider a line which is rotated in the negative direction by 10^{o}. Neglecting the absorption that takes place since the polarizers are no longer crossed, a rotation of the polarizer to + 10^{o} will make the radiation from this line have its plane of polarization perpendicular to the plane of the analyzer and this line then should not be seen. All of the magnetic rotation spectra were obtained in this manner.

3-0 Band

The 3-0 band of nitric oxide is located at approximately 1.8 μ. This band has been investigated extensively for three reasons: the grating used has 6,000 lines/cm and is blazed at about 27° or 1.5 μ in the first order, the Lead Sulphide detector has a relatively high efficiency at 1.8 μ, and the 300 watt Zirconium arc gives a good amount of radiation at 1.8 μ.

The P and R branch lines were obtained in magnetic rotation using slits 100 and 150 μ wide, corresponding to .60 wave numbers.

Gas pressures from 1 to 18 cm of mercury were used in the multiple traverse cell, giving absorbing paths ranging from .1 to 2 meter-atmospheres. It was found that pressures in excess of 20 cm of mercury caused the magnetic rotation spectrum in the P and R branches to disappear. This is probably due to self-absorption as mentioned on page 25.

The P branch in the 3-0 band has both sub-band components well resolved, while in the R branch the sub-bands are not resolved at the slit widths that were used. The magnetic rotation spectra were obtained for the above pressures first with the polaroids in the crossed position and then set at progressively larger positive and negative

angles until the P branch showed absorption for one component and rotation for the other component. It was not possible to determine with high accuracy the frequencies in the P and R branch lines for the magnetic rotation spectra. Only the direction of rotation for the components was determined.

The magnetic rotation spectrum of the Q branches were obtained using slits of 25 and 30 μ, which corresponds to .12 wave numbers. With slits of this size it was possible to run the fringe calibration system and the magnetic rotation spectra simultaneously. This allowed a fairly accurate determination of the frequencies for those lines in the Q branches which are rotated. The Q branch rotations were obtained using a gas pressure of 56 cm of mercury in the multiple traverse cell, giving a total absorbing path of about 6 meter-atmospheres.

The magnetic rotation spectra for the Q branches were taken by starting at the $R_1(3/2)$ line with the polaroids at $\pm$ 25°. When the $R_1(1/2)$ line had been recorded the polaroids were turned to the crossed position or to the angle, either positive or negative, that was desired and the Q branches examined for magnetic rotation at this setting. After the Q branches had been observed, the polaroids were returned to the original setting and

two P branch lines recorded. The frequencies of the R and P branch lines are known and with the aid of the fringe calibration system the frequencies for the rotated lines in the Q branches were obtained.

2-0 Band

The 2-0 band of nitric oxide is located at approximately 2.7μ . Only the Q and R branches of this band have been observed. This is due to the rapid decrease in sensitivity of the instrument in this region. The decrease in sensitivity can be attributed to the following reasons: both the Zirconium arc and the Lead Sulphide detector have envelopes which become absorbing around 2.7μ , a Germanium filter must be used in order to absorb the radiation below 2μ , and the grating that was used for these spectra had to be employed at an angle far from the blaze of the grating.

In order to observe the 2-0 band the slits had to be opened to 200 and 250μ , corresponding to .28 wave numbers. Pressures of 10 cm of mercury were used which gave an absorbing path of about 1 meter-atmosphere. Only the direction of rotation for the sub-bands could be determined for the 2-0 band. With the 2-0 band we have direct evidence of the direction of rotation of the individual R branch sub-bands since several of these lines are well resolved.

RESULTS AND DISCUSSION

3-0 Band

As has been mentioned previously, relatively large slit widths were necessary in order to obtain the magnetic rotation spectrum of the P and R branches in the 3-0 band. In order to determine which lines appeared in the magnetic rotation spectrum, the following procedure was employed. An overlay was obtained for the P and R branch lines and the components marked so that the magnetic rotation lines could be identified by their J number. The absorption spectrum of the 3-0 band is shown in Figure 10. The next three figures (11, 12 and 13)show typical magnetic rotation spectra. The angular notation on these figures gives the angle between the planes of polarization from the crossed position.

Here one notices an interesting phenomenon. In the R branch, the line at J = 19/2 is missing in magnetic rotation and as the angle is increased in the positive or negative direction, the absorption for this line is greater than that of any other R branch line. If one examines the curves for the Zeeman splittings shown in Figure 4, it will be noted that the Zeeman splitting for J = 19/2 in the $^2\pi$ 3/2 state is almost 0. Since this

line is missing from the magnetic rotation spectrum, we have here an experimental indication that the magnitude of the magnetic rotation depends upon the magnitude of the Zeeman splitting.

If the R(19/2) line is missing then one would expect that a similar line, P(21/2), should also be missing. This, however, is not the case. We have already seen that the magnetic rotation spectra depends upon the magnitude of the Zeeman splitting. It is also dependent upon the strength of the ordinary absorption line since the change in the index of refraction is dependent upon the magnitude of the absorption. Since the P(21/2) line is visible in magnetic rotation and the Zeeman splitting for this line is small, then the absorption for this line must be large. This, in fact, is true. While studying the fundamental of $N^{15}O$, Fletcher and Begun[17] observed the P(21/2) line due to the presence of 6% of $N^{14}O$ and only the P(21/2) line was observed. We have also noticed that the P(21/2) line for the $^2\pi_{1/2}$ component is abnormally large as can be seen in Figure 10a.

One can easily determine the direction of rotation for the sub-band components in the P branch since they are well resolved. The rotation is negative for the $^2\pi_{1/2}$

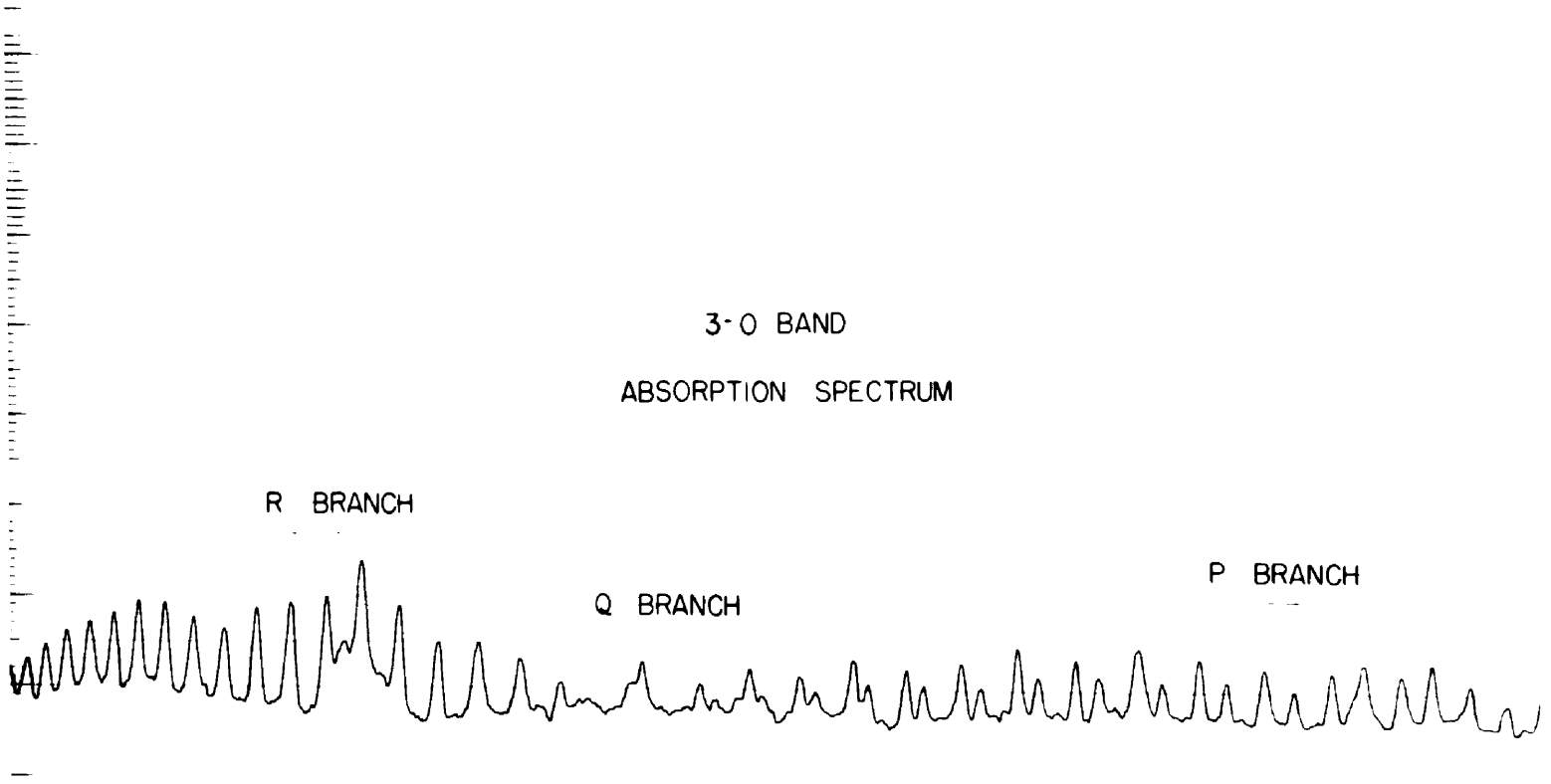

Figure 10

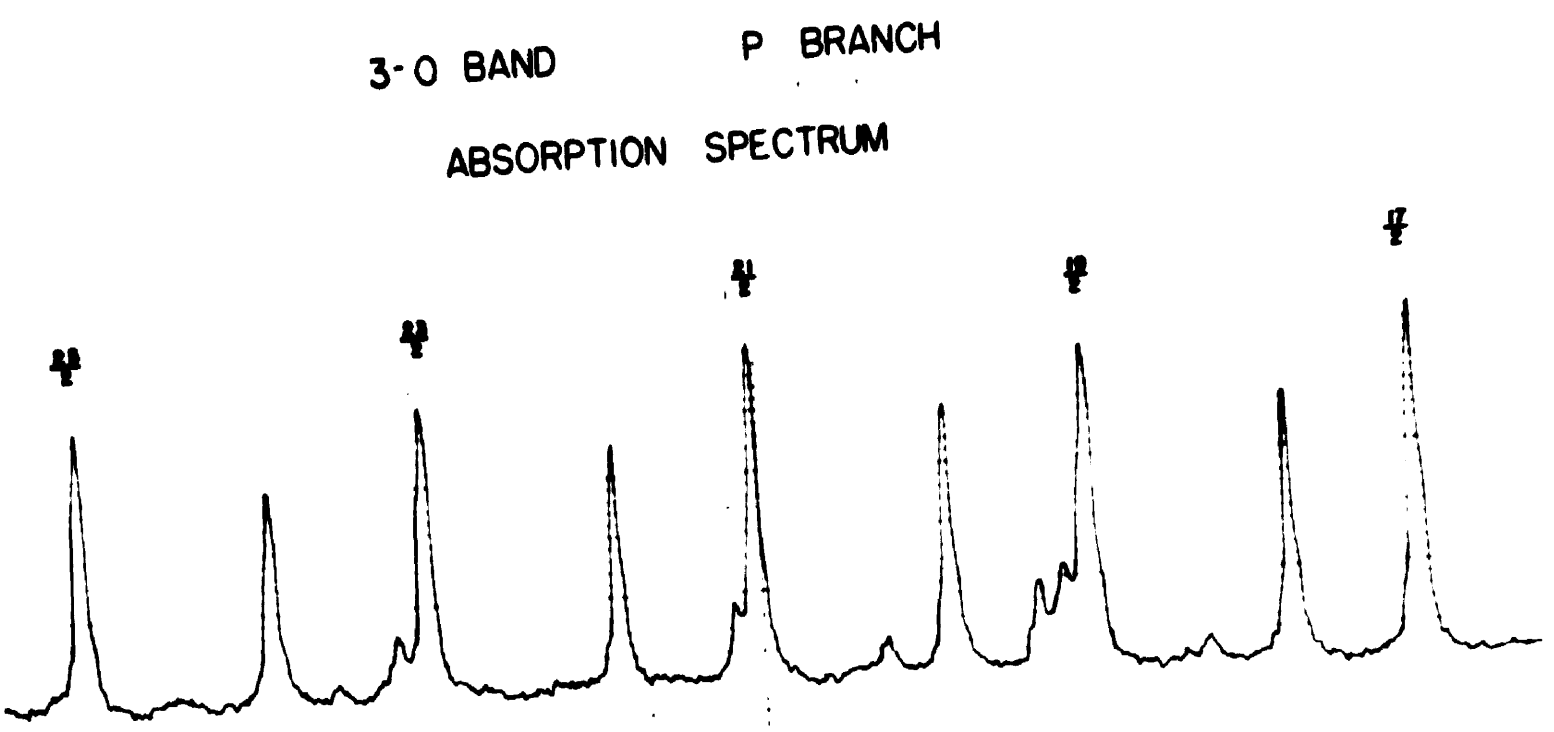

The numbers indicate $^2\Pi_{1/2} \leftarrow {}^2\Pi_{1/2}$ transitions

Figure 10a

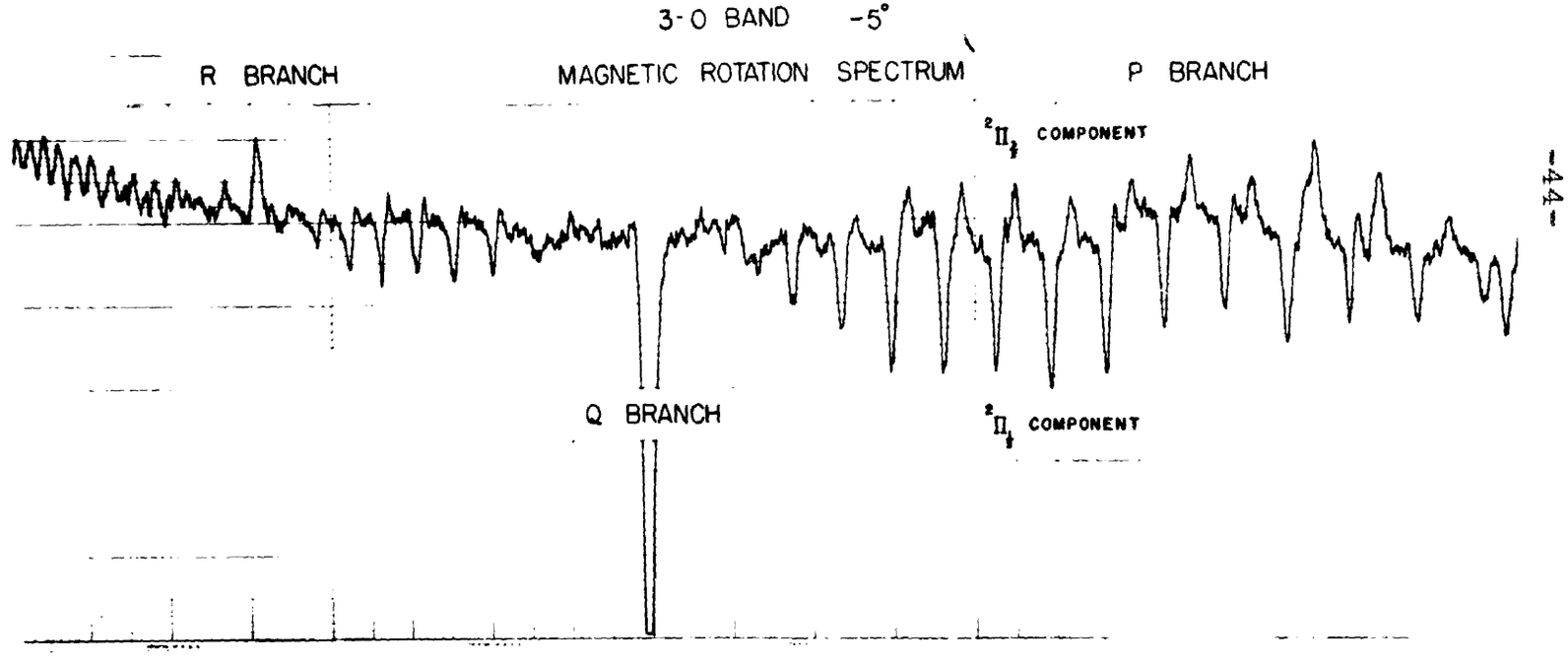
3-0 BAND -5°
R BRANCH
MAGNETIC ROTATION SPECTRUM
P BRANCH
$^2\Pi_{\frac{3}{2}}$ COMPONENT
Q BRANCH
$^2\Pi_{\frac{1}{2}}$ COMPONENT

Figure 11

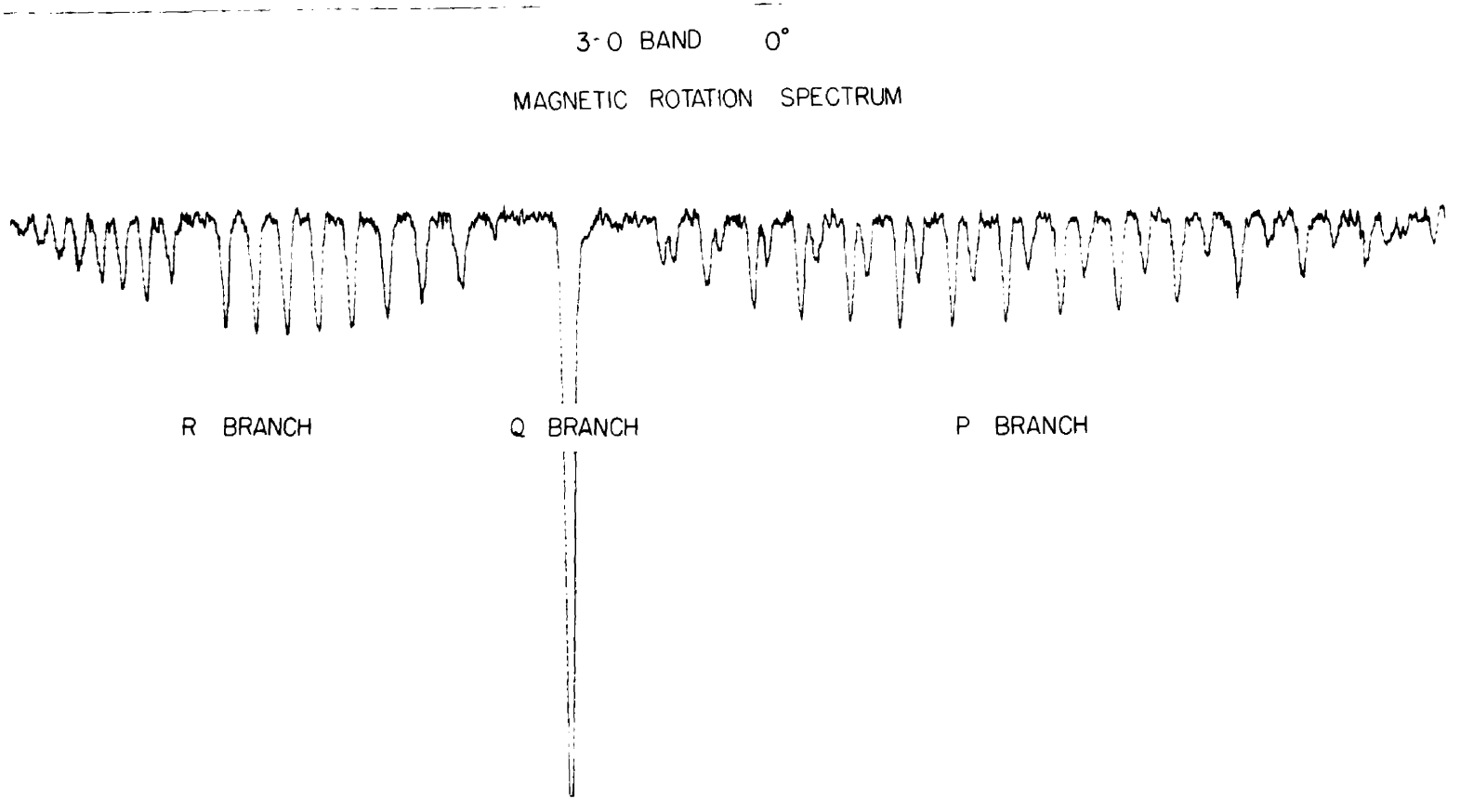
3-0 BAND 0°
MAGNETIC ROTATION SPECTRUM
R BRANCH
Q BRANCH
P BRANCH

Figure 12

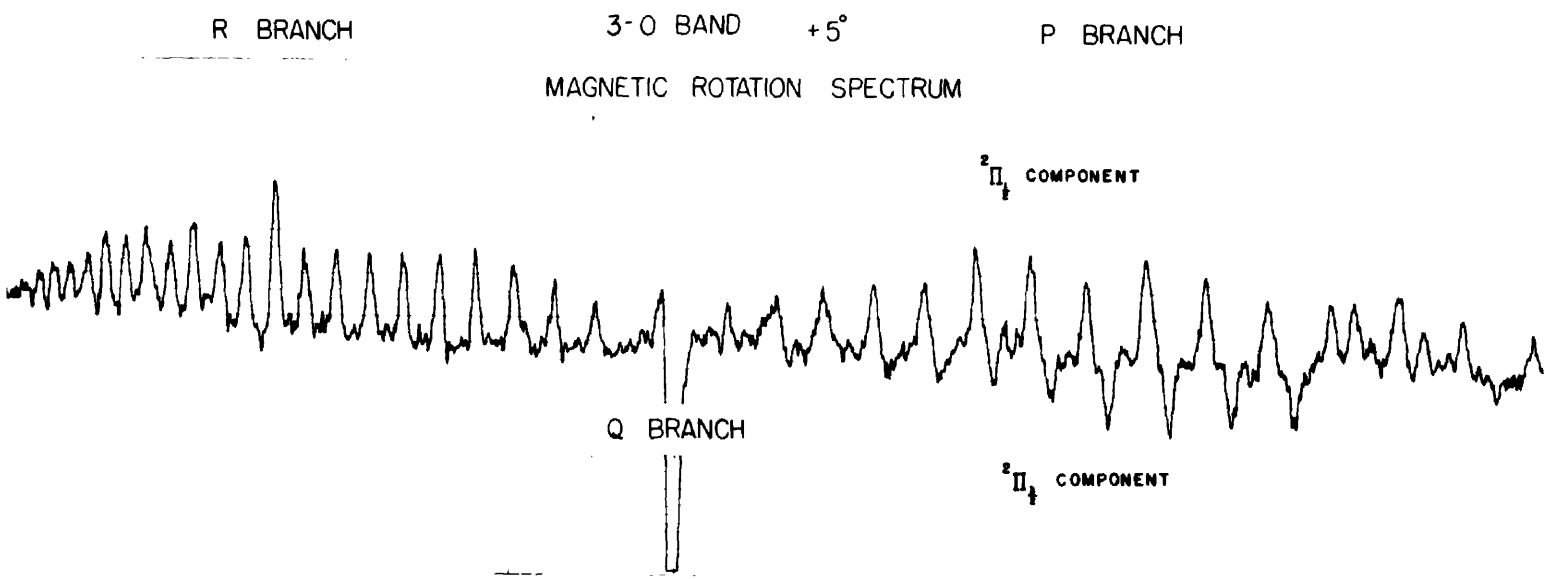
R BRANCH
3-0 BAND +5°
P BRANCH
MAGNETIC ROTATION SPECTRUM
$^2\Pi_{\frac{1}{2}}$ COMPONENT
Q BRANCH
$^2\Pi_{\frac{1}{2}}$ COMPONENT

Figure 13

components and positive for the $^2\pi_{3/2}$ components. By using the missing line at R = 19/2, it is possible to deduce the direction of rotation for the sub-band components in the R branch even though they are not resolved. From the absorption spectrum it is known that the absorption for the $^2\pi_{1/2}$ component is much stronger than for the $^2\pi_{3/2}$ component.

Knowing the above facts, one can say that the direction of rotation which gives the maximum absorption for the R(19/2) line corresponds to the P branch line which becomes weaker in rotation for this same direction. This component in the P branch turns out to be the $^2\pi_{1/2}$ component. Thus, the R branch lines corresponding to $^2\pi_{1/2}$ transitions show negative rotations, while the R components for the $^2\pi_{3/2}$ transitions show positive rotations.

The Q branch rotation seen for these wide slit openings and for the two directions of rotation of the polarizer indicate that the Q component may show both positive and negative rotations. Since the Q branch was much stronger than any of the other rotations, it was possible to narrow the slits and examine its structure. The strength of the Q branch in magnetic rotation may possibly be explained by its Zeeman splitting. The

Q branch is formed by transitions occurring for $\Delta J = 0$. This then means that all the Zeeman components will have the same frequency shift. Thus, the Zeeman pattern for any one Q branch line will appear to have only two components. Also, the splitting for the Q branch lines is larger than that for any of the P or R branch lines.

The next eight figures show the Q branch in magnetic rotation with narrow slit widths. Figure 14 is the normal absorption for the Q branches. The next seven figures (15 - 21) show the Q branches in magnetic rotation for crossed polaroids and plus and minus directions of rotation of the polarizer. These magnetic rotation curves are composite curves. When the polaroids are not in the crossed position, some radiation is transmitted by the analyzer. Thus, there will be some absorption taking place along with the magnetic rotation that is observed.

It was decided, therefore, to run absorption curves for the Q branches at the same angles to be observed in magnetic rotation. If these absorption curves are then subtracted from the curves obtained with the field, what remains should be a true picture of the magnetic rotation in the Q branches. These are the curves that are shown in Figures 15 through 21.

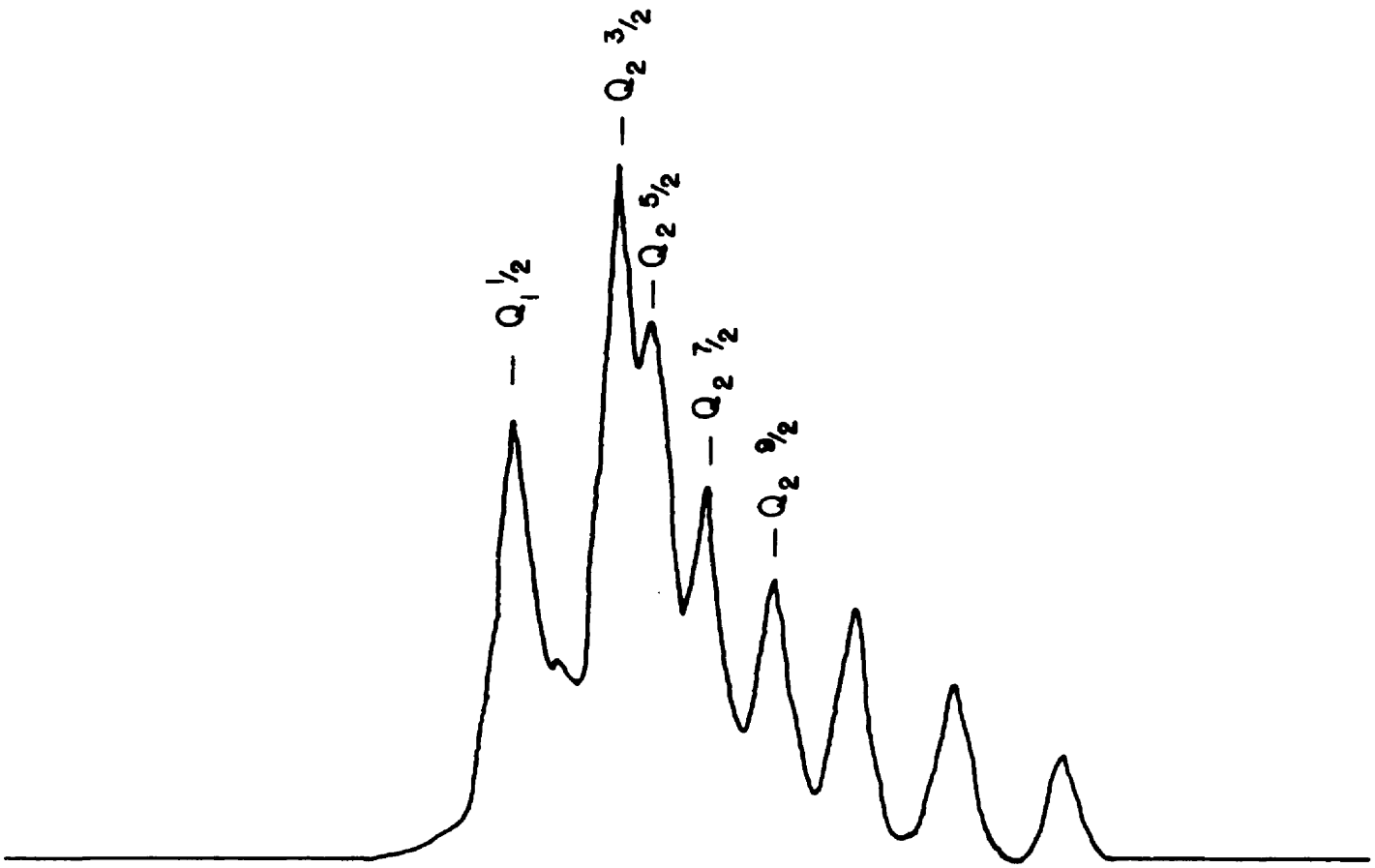

Q BRANCH ABSORPTION

FIGURE 14

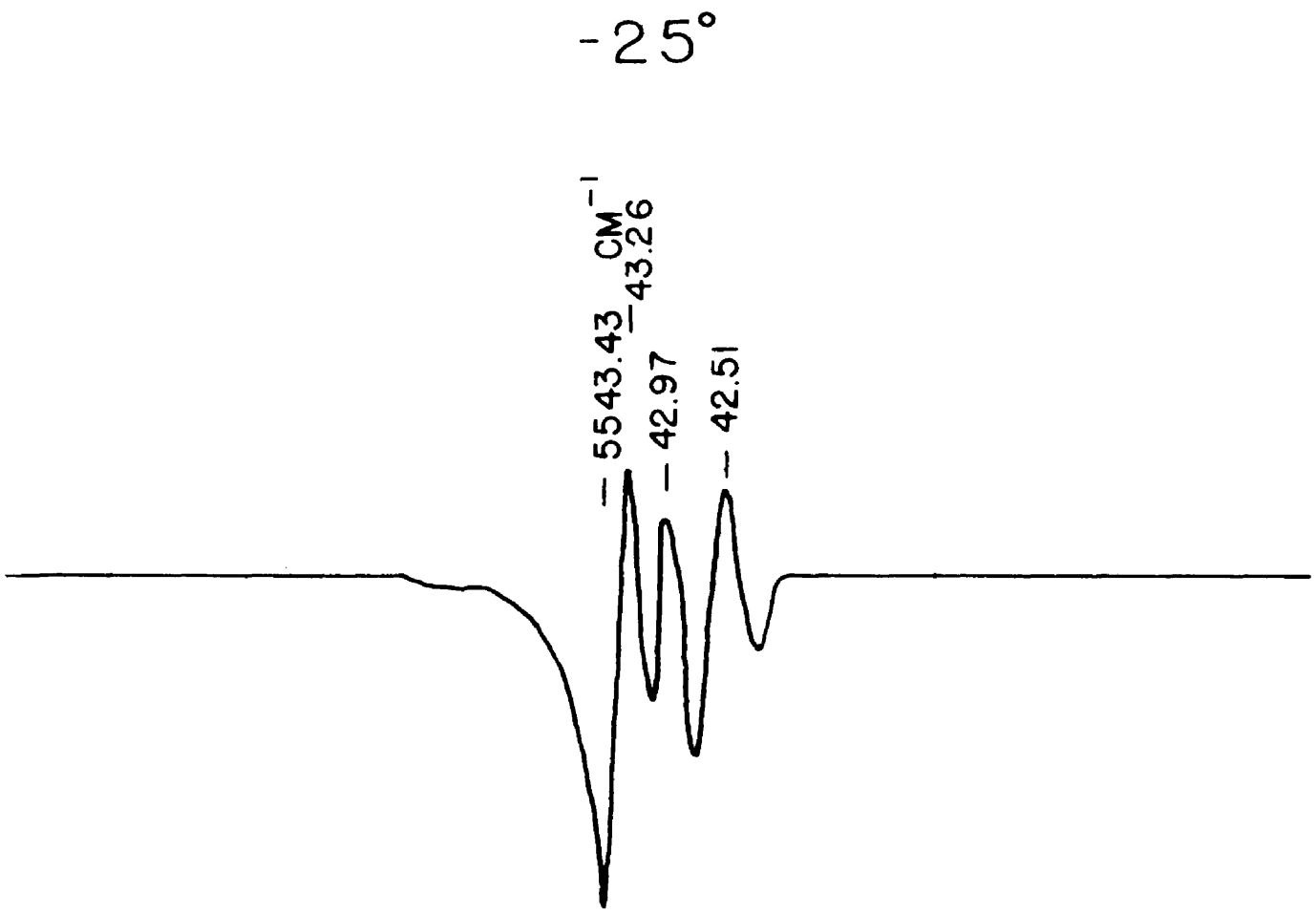

FIGURE 15

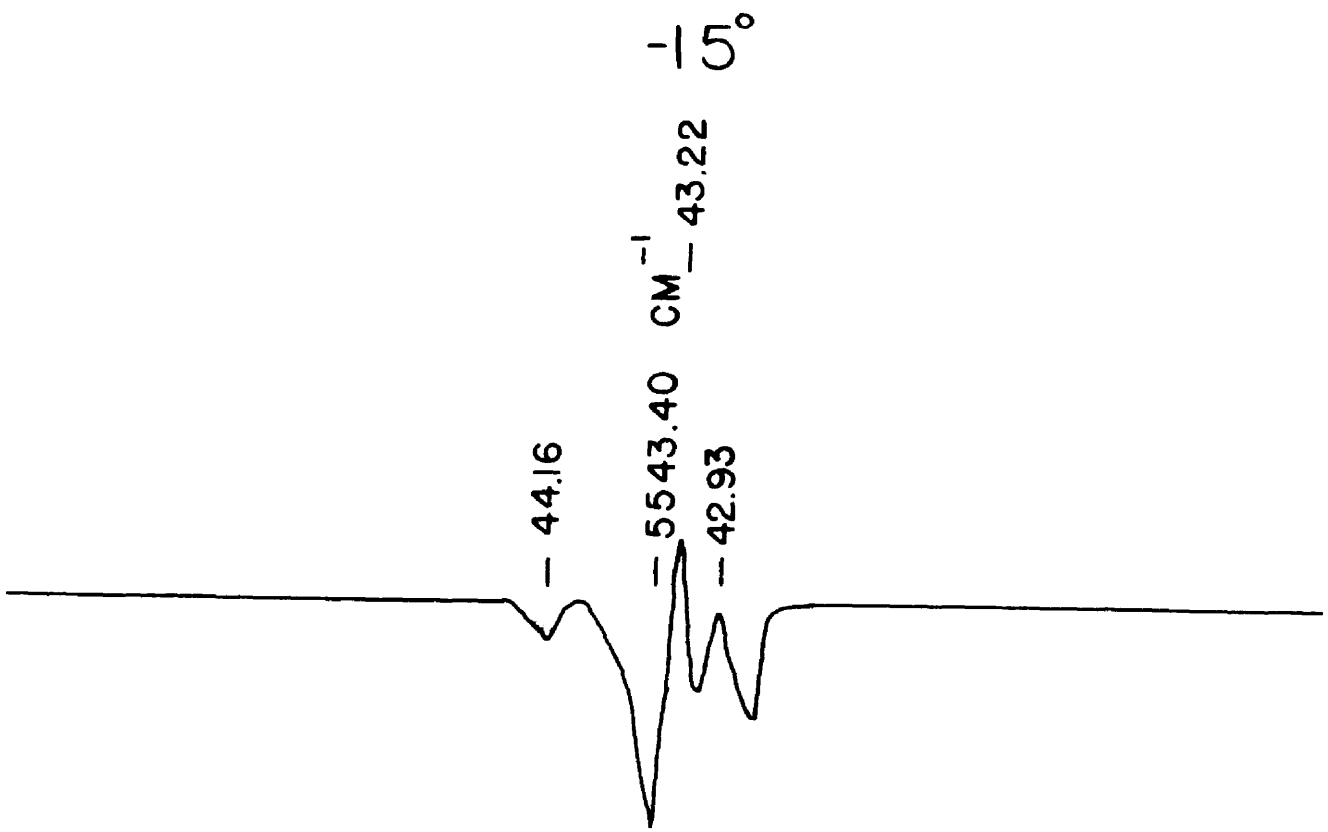

FIGURE 16

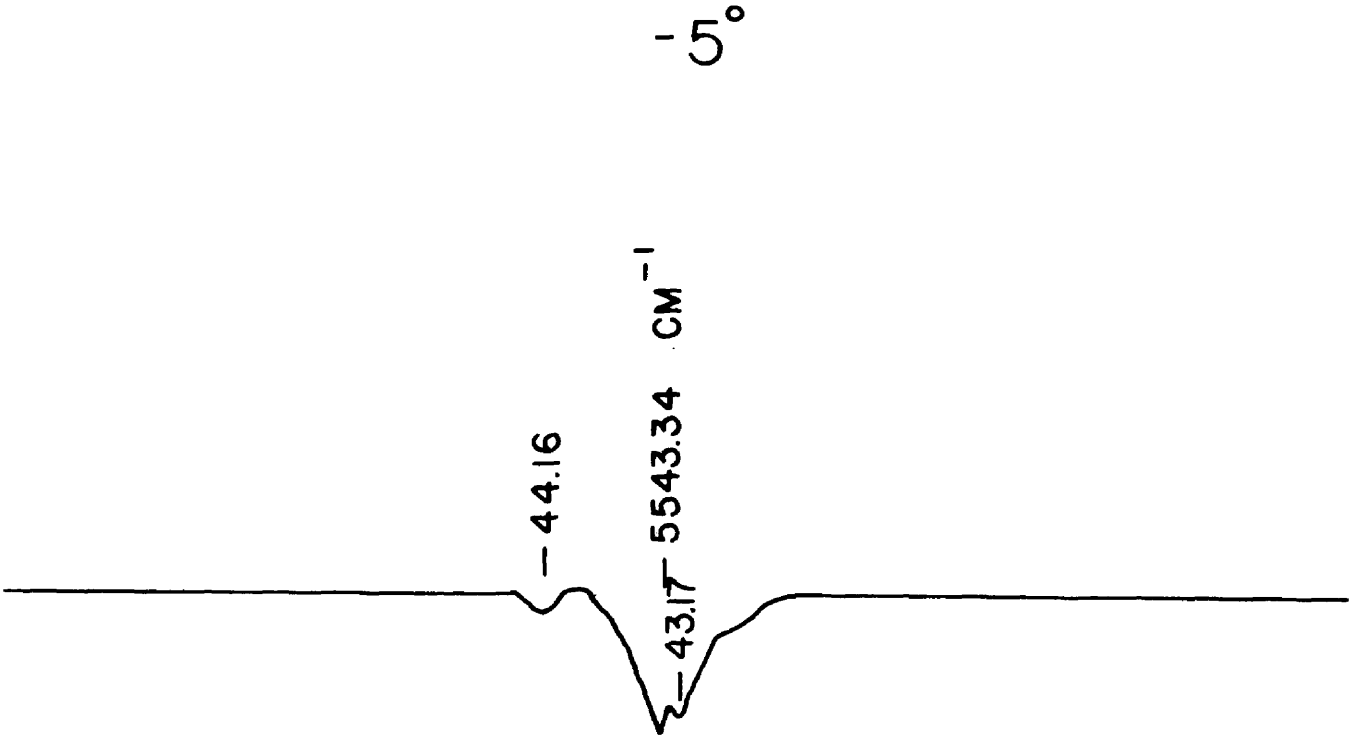

FIGURE 17

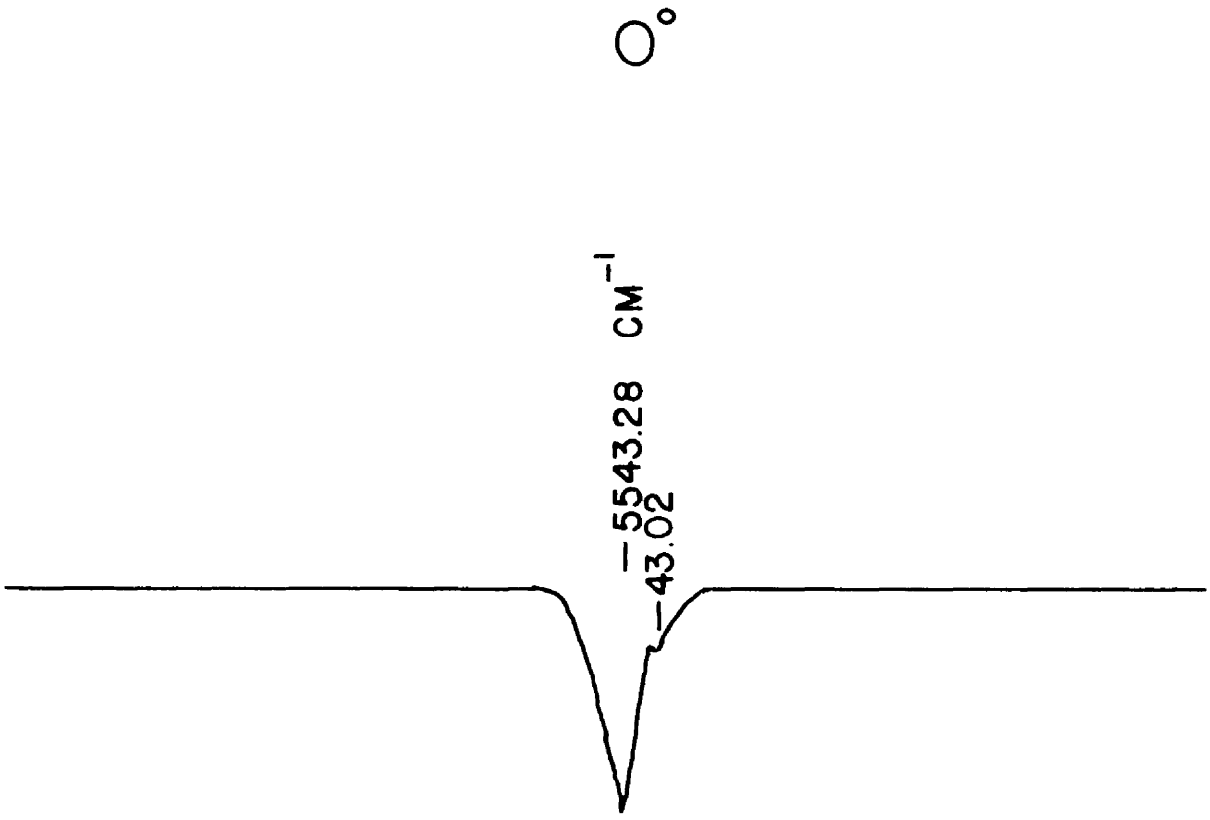

FIGURE 18

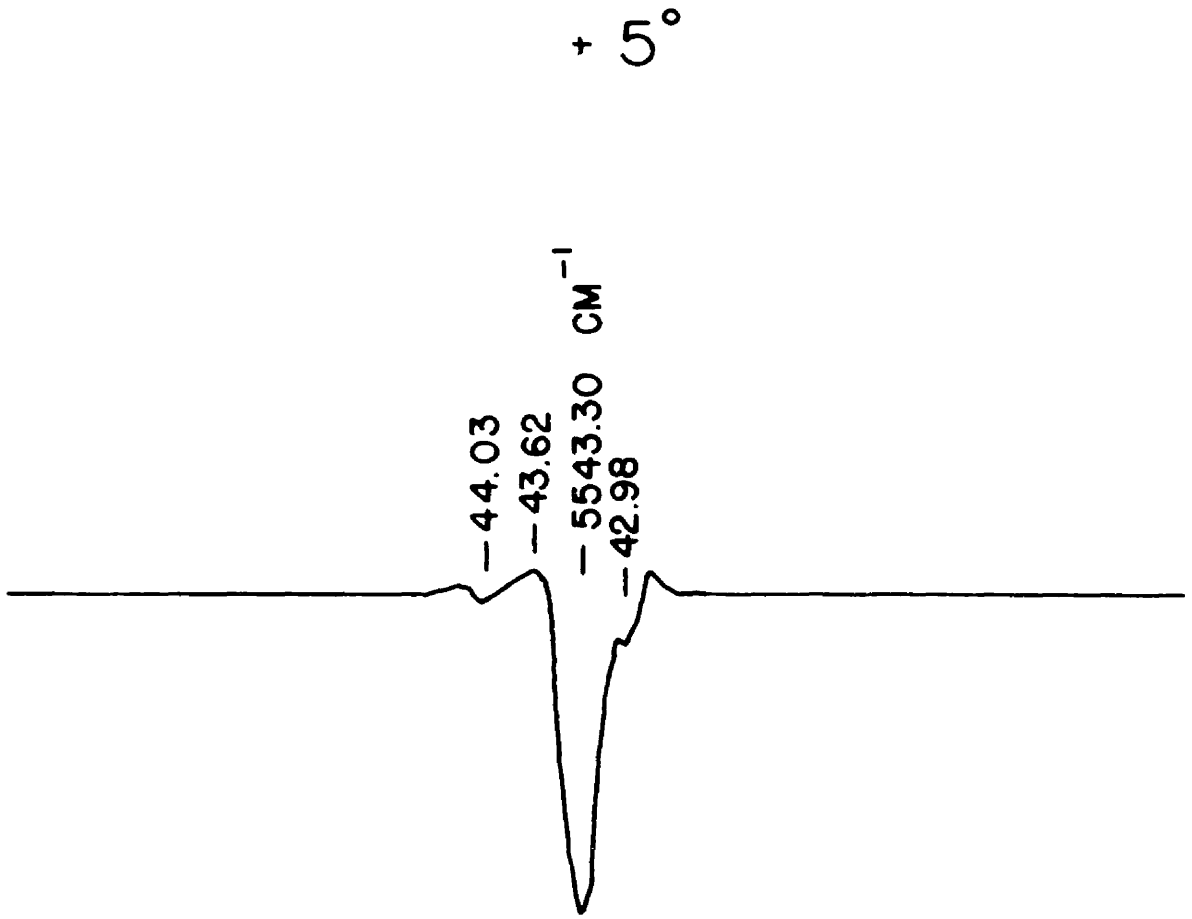

FIGURE 19

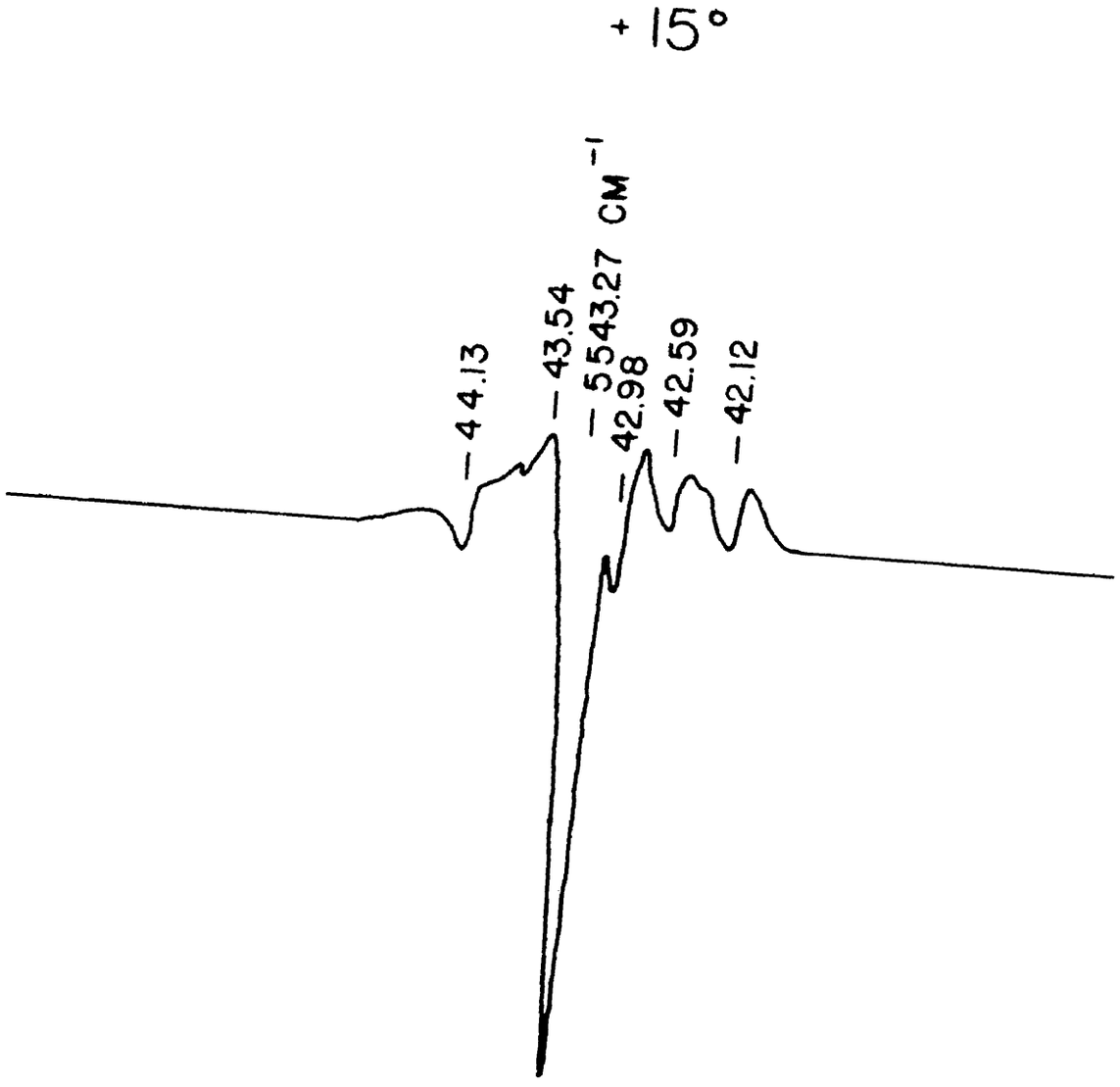

FIGURE 20

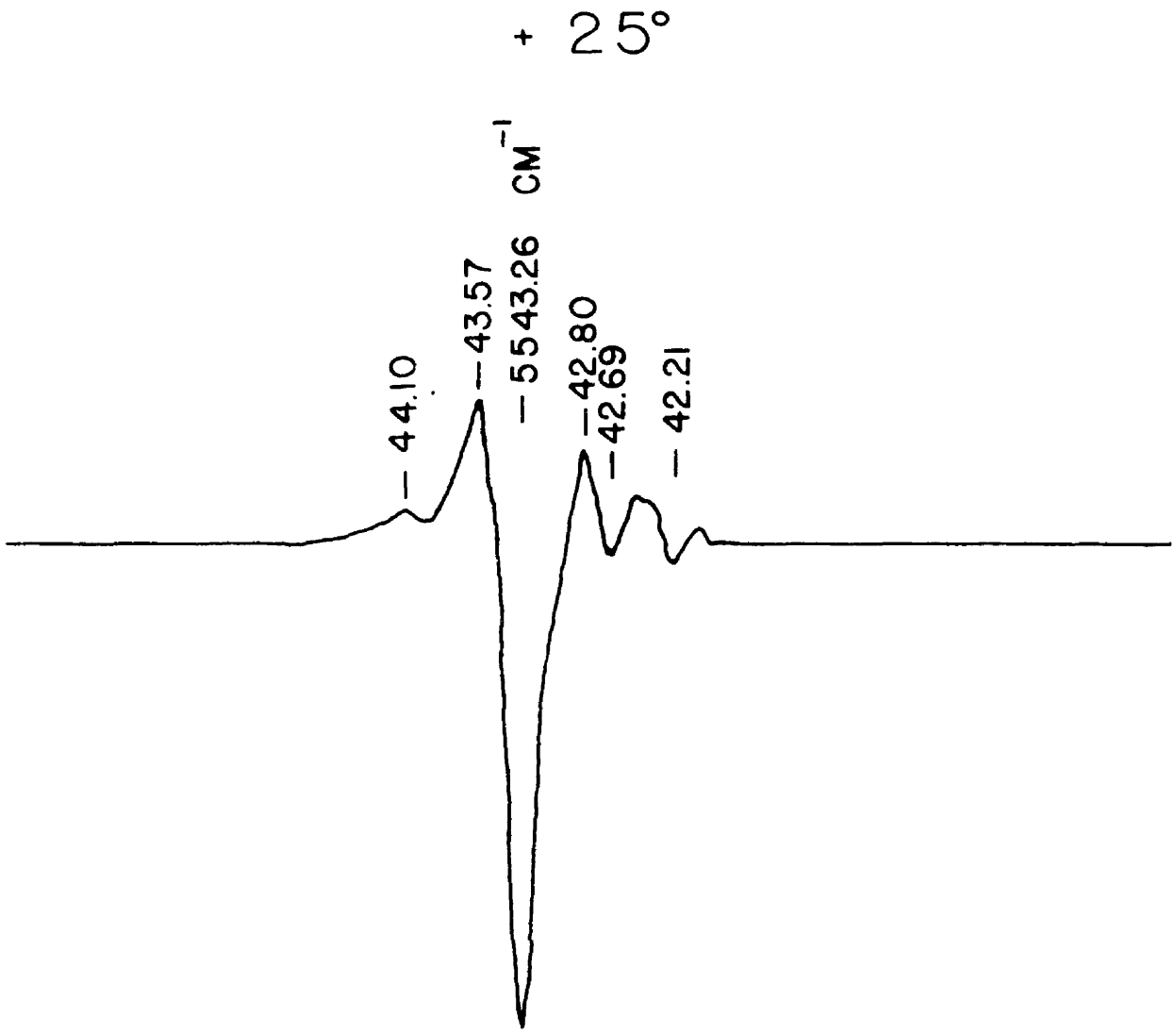

FIGURE 21

Normal Spectrum

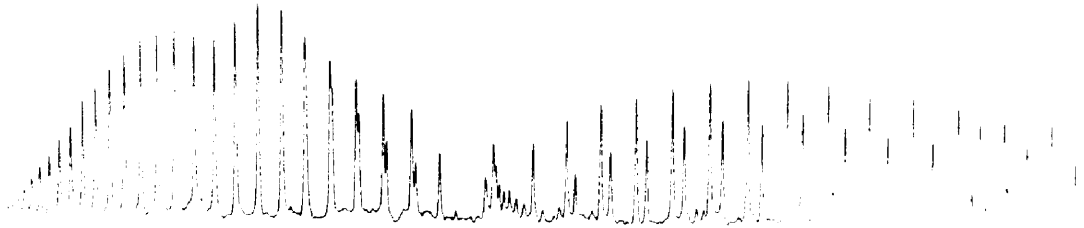

Zeeman Spectrum

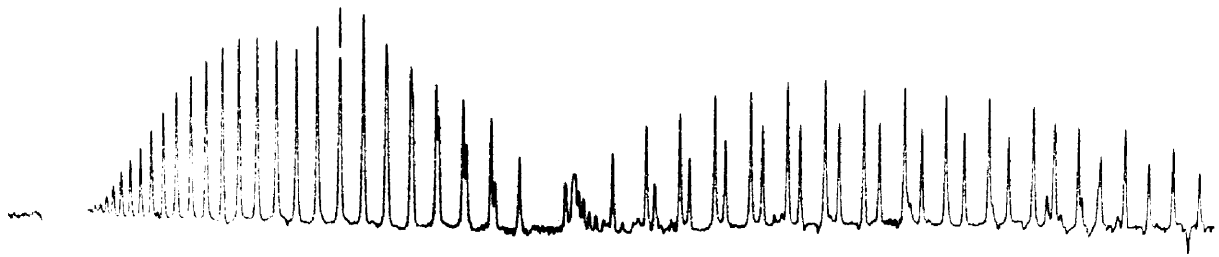

Figure 22

Since good signals could be obtained for the Q branches with narrow slits, it was possible to use the fringe calibration system at the same time and thus determine the frequency of the magnetic rotation lines observed. Table 1 gives the theoretical frequencies obtained by using constants determined for the 3-0 band by Van Horne[18] and the frequencies observed experimentally in magnetic rotation.

It can be seen that the direction of rotation for the Q branch arising from $^2\pi_{3/2}$ component is positive, while the direction of rotation for the Q branch arising from the $^2\pi_{1/2}$ component is negative. Thus, for the 3-0 band the $^2\pi_{1/2}$ state components are rotated in a negative direction while the $^2\pi_{3/2}$ state components are rotated in the positive direction.

TABLE I

Theoretical Frequencies for Q Branches

Q_1 $^2\pi_{1/2} - {}^2\pi_{1/2}$

5544.12 cm^{-1}
43.97
43.71
43.34
42.88

Q_2 $^2\pi_{3/2} - {}^2\pi_{3/2}$

5543.29 cm^{-1}
43.03
42.65
42.17
41.59
40.89

Observed Frequencies for Magnetic Rotation Lines in the Q Branches

Q_1 $^2\pi_{1/2} - {}^2\pi_{1/2}$

5544.16 cm^{-1}
43.39

Q_2 $^2\pi_{3/2} - {}^2\pi_{3/2}$

5543.28 cm^{-1}
42.99
42.64
42.17

2-0 Band

For the P and R branch lines in the 2-0 band the same procedure was followed as outlined in the preceding section. First, a normal absorption spectrum (Figure 23) was obtained of the 2-0 band at the slit widths used for magnetic rotation and by referring to the work done by Nichols[19], the components were identified. A tracing of this band was then made so that it could be used as an overlay to determine which components were rotated by the magnetic field for the 2-0 band. Figures 24, 25, and 26 show typical magnetic rotation spectra. The angular notation of these figures gives the angle between the planes of polarization from the crossed position. It is easy to see that the $^2\pi_{1/2}$ components in the R branch are rotated in the negative direction and that the $^2\pi_{3/2}$ components are rotated in the positive direction.

It will be noted that there is a strong rotation in the R branch for the line $J = 5/2$. If the amount of rotation is dependent upon the magnitude of the Zeeman splitting and the intensity of the absorption line, one would expect a fairly large signal for the $J = 3/2$ line also. Instead, there is only a small amount of rotation present. Unfortunately there is a very strong water absorption line at $J = 3/2$, thereby hiding this line.

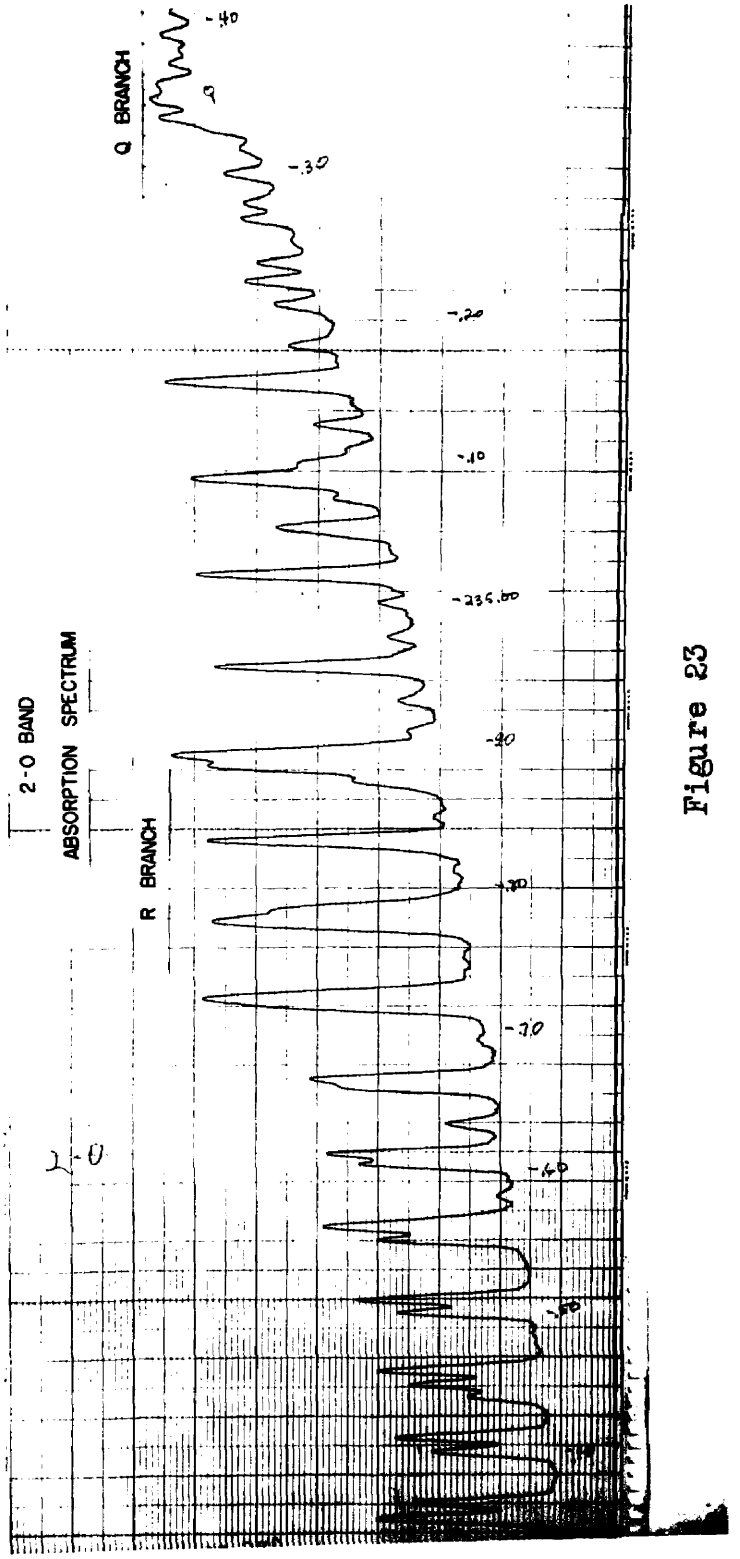
2-0 BAND
ABSORPTION SPECTRUM
Q BRANCH
R BRANCH
-40
-30
-20
-10
-235.00
-50
-30
-70
-40
-60
J-0

Figure 23

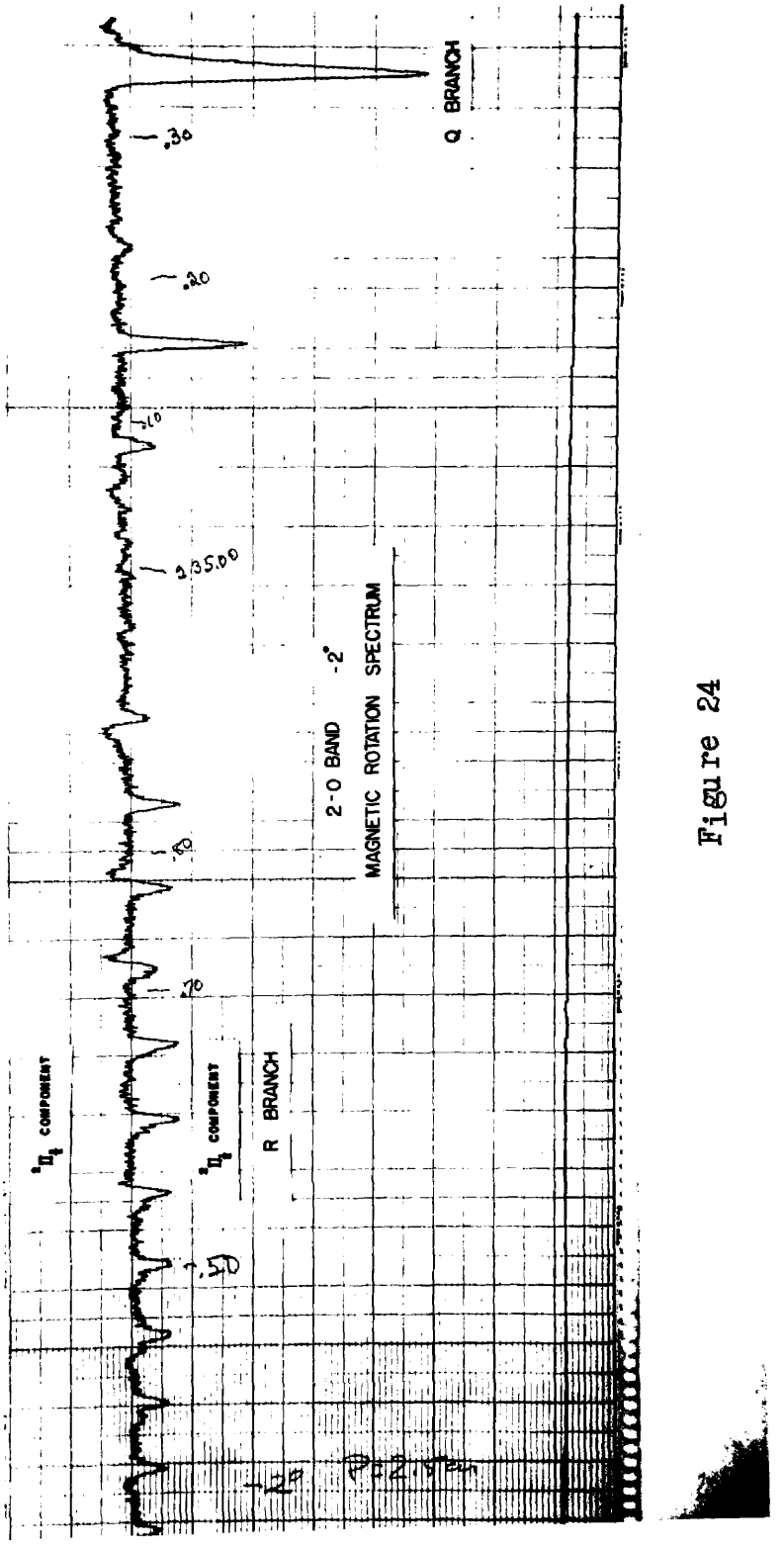
Q BRANCH
.30
.20
.10
3305.00
.80
.70
2-0 BAND -2°
MAGNETIC ROTATION SPECTRUM
$^2\Pi_{\frac{1}{2}}$ COMPONENT
$^2\Pi_{\frac{3}{2}}$ COMPONENT
R BRANCH

Figure 24

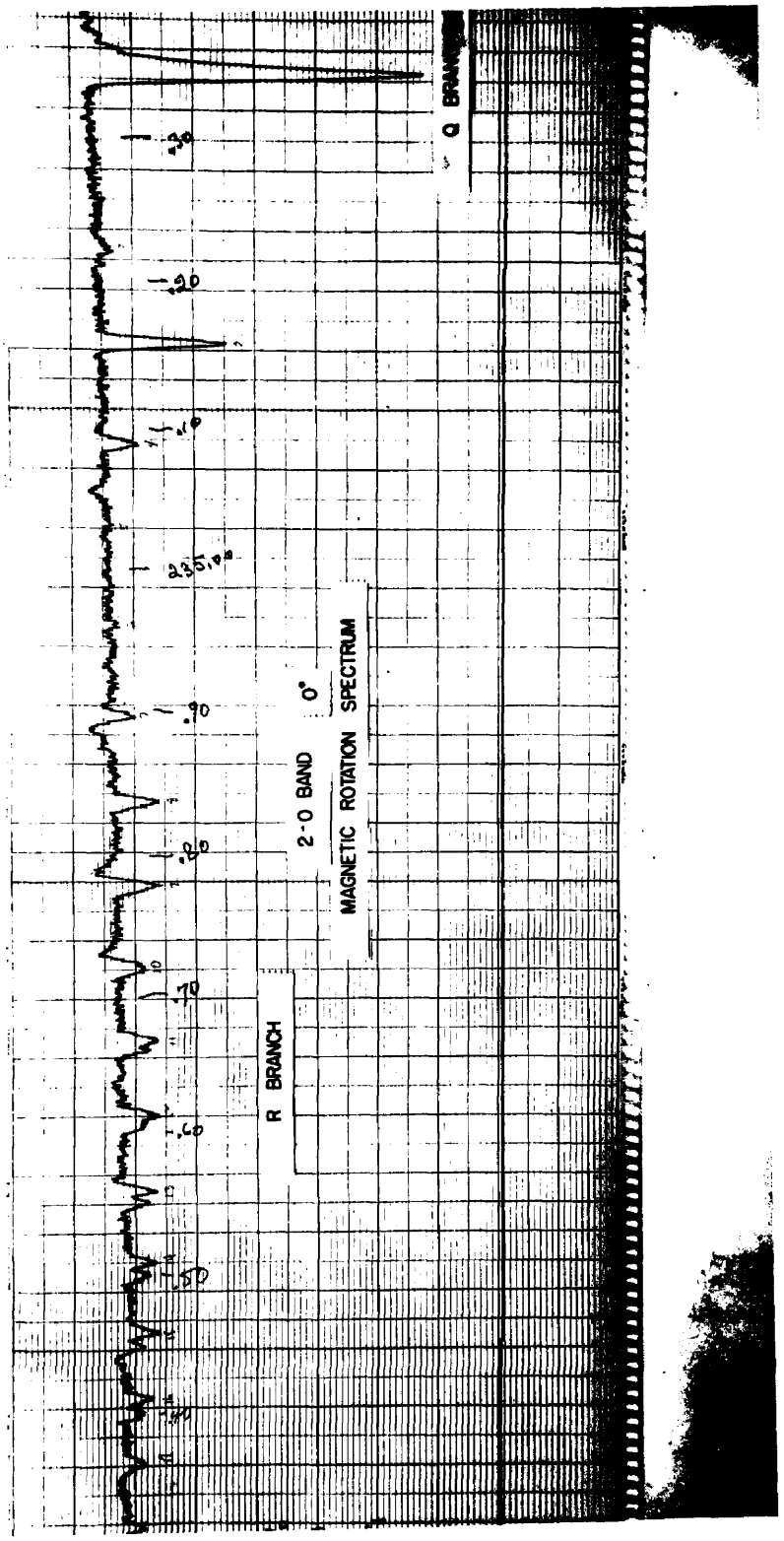

Figure 25

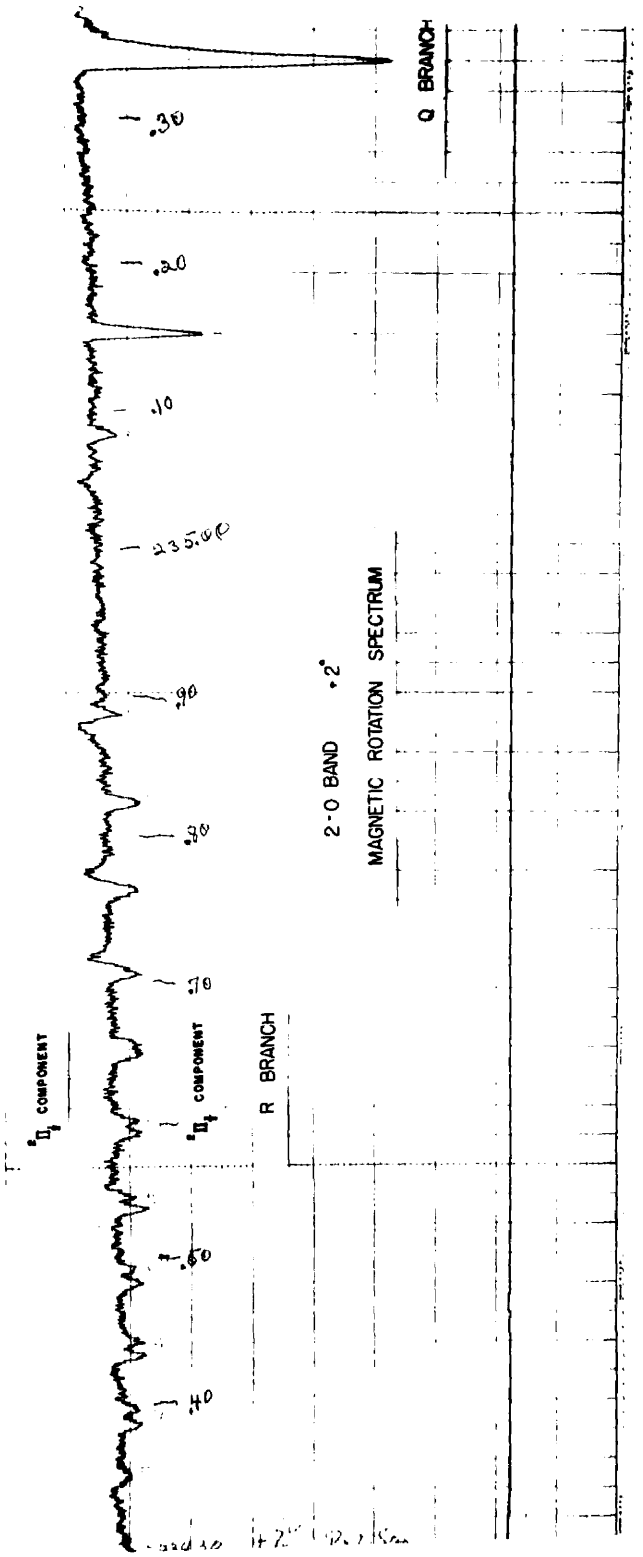
Q BRANCH
.30
.20
.10
2350
.90
.80
.70
.60
.40
2-0 BAND .2°
MAGNETIC ROTATION SPECTRUM
R BRANCH
$^2\Pi_{\frac{1}{2}}$ COMPONENT
$^2\Pi_{\frac{3}{2}}$ COMPONENT

Figure 26

The signal for the Q branch shows little variation in magnitude for the amount of rotation shown here. This possibly indicates that the Q branch has at least two components with opposite rotations. Also, this signal is much larger than the signal for any other line in the 2-0 band. The explanation for this is probably the same as for the large signal seen in the Q branch of the 3-0 band and if an examination of this Q branch had been possible with narrow slits, rotation similar to that seen in the 3-0 band Q branch would probably have been observed.

CONCLUSION

A close examination of the magnetic rotation spectra as a function of the angle of the polarizers shows that the rotation follows very closely the curves for the magnitude of the Zeeman splitting and the absorption spectrum, indicating the form of the Verdet constant given by Serber is close to the experimental result seen for nitric oxide. Unfortunately, this result cannot be applied directly to NO since the Zeeman splitting and the amplitudes cannot be simply stated for a case of intermediate coupling. Additional theoretical work needs to be done on this problem. More experimental work should be done to try to establish the J dependence for the magnitude of the rotation.

Nitric oxide is often referred to as having no magnetic moment in the ground state or upper states for the $^2\pi_{1/2}$ component. There is observable, however, rotation for the R(1/2) line in the 3-0 band for small angles of rotation of the polarizer indicating that there must be a magnetic moment for the $^2\pi_{1/2}$ state, probably due to the beginning of spin uncoupling, even for this small amount of rotational energy. In order to confirm this idea the magnetic rotation spectrum of NO in the fundamental should be investigated, with particular attention being paid to the R(1/2) line.

BIBLIOGRAPHY

1. Macaluso, P., and O. M. Corbino. Sur Une Novvelle Action Subie par la lumière Traversant Certainos Vapeurs Métalliques dans un Champ Magnétique. Compt. Rend. 127, 548 (1898).

2. Wood, R. W. The Resonance and Magnetic Rotation Spectra of Sodium Vapor Photographed with the Concave Grating. Astrophys. J. 30, 339 (1909).

3. Righi, A. Sur l'Absorption de la lumière produite par un Corps Placé dans un Champ Magnétique. Compt. Rend. 127, 216 (1898).

4. Loomis, F. W. Phys. Rev. 40, 380 (1932); 46, 286 (1934).

5. Carroll, T. Magnetic Rotation Spectra of Diatomic Molecules. Phys. Rev. 52, 822 (1937).

6. Herzberg, G. Spectra of Diatomic Molecules, ed. 2, D. VanNostrand Co., Inc., New York (1950) page 218.

7. Hill, E., and J. H. VanVleck. On the Quantum Mechanics of the Rotational Distortion of Multiplets in Molecular Spectra. Phys. Rev. 32, 250 (1928).

8. Herzberg, G. reference 6, page 343.

9. Somerfeld, A. Wave-Mechanics. Methusen & Co. LTD., London (1930) page 169.

10. Somerfeld, A. Optics. Academic Press, Inc., New York (1954) page 98.

11. Hill, E. On the Zeeman Effect in Doublet Band Spectra. Phys. Rev. 34, 1507 (1929).

12. Crawford, F. H. Zeeman Effect in Diatomic Molecular Structure. Rev. Mod. Phys. 6, 90 (1934).

13. Noble, R. H. A vacuum spectrograph for the infrared. J. Opt. Soc. Am. 43, 330 (1953).

14. Brown, R. G. The Infrared Spectrum of Methyl Chloride in the 1.6 Micron Region. M.S. Thesis, Michigan State University (1957).

15. Van Horne, B. H. The Near Infrared Spectra of Deuterium Chloride and Nitric Oxide. Ph.D. Thesis, Michigan State University (1957).

16. Polaroid Corporation. Polarizers for the Near Infrared. Polaroid Reporter, No. 1, page 2 (1951).

17. Fletcher, W. H., and G. M. Begun. Fundamental of $N^{15}O$. Journ. Chem. Phys. 27, 579 (1957).

18. Van Horne, B. H. reference 15.

19. Nichols, N. L. The Near Infrared Spectrum of Nitric Oxide. Ph.D. Thesis, Michigan State College (1953).

20. Serber, R. The Theory of the Faraday Effect in Molecules. Phys. Rev. 41, 489 (1932).